Tectonic evolution of the Colorado Basin, offshore Argentina, inferred from seismo-stratigraphy and depositional rates analysis

Markus J. Loegering, Z. Anka, Julia Autin, Rolando Di Primio, Denis Marchal, Jorge F. Rodriguez, D. Franke, Eduardo Vallejo

Tectonic evolution of the Colorado Basin, offshore Argentina, inferred from seismo-stratigraphy and depositional rates analysis .

M. J. Loegering[(1,*)], Z. Anka[(1)], J. Autin[(1, **)], R. di Primio[(1)], D. Marchal[(2)], J. F. Rodriguez[(2)], D. Franke[(3),] Eduardo Vallejo (2)

[(1)] GFZ German Research Centre for Geosciences, Germany
[(2)] Petrobras Argentina
[(3)] Federal Institute for Geoscience and Natural Resources (BGR), Germany
(*) Now at: Fugro-Robertson Ltd., UK
(**) Now at: Université de Strasburg, France

Abstract

Based on a dense 2D seismic reflection dataset and 8 exploration wells, we reinterpreted the geological evolution of the Colorado Basin. The basin is located on the continental shelf and slope within 50 to 2250 m of bathymetry. The total sediment fill can be up to 16,000 m. Seismic-to-well log correlations provide a chrono-stratigraphic framework for the interpreted sesmic sequences. We show that the Colorado Basin records the development of a Permian pre-rift period, a Triassic/Jurassic to Early Cretaceous rift phase and a Lower Cretaceous to Tertiary drift phase. This passive margin represents the evolution of lithospheric extension from active rifting to the thermal subsidence/drift stage. Several Cretaceous to Cenozoic slumping episodes were identified and related to progradation of the sequences and sediment build-up in the slope, as well as to the development of seaward dipping extensional faults.

Assuming an accumulation time span of 25 Ma for the syn-rift succession, which correspond to the duration of extensional phases preceding the final break-up of the South Atlantic, sedimentation rates are in the order of 118 m/Ma. By Late Cretaceous, the Gondwana break-up had stopped in almost all areas and post-rift thermal subsidence dominated the basin development. During the early phase of subsidence, high sedimentation rates of up to 122 m/Ma are recorded. An important decrease of sediment supply (30 m/Ma) occurred until the end of the sag phase during the deposition of the Colorado Formation and sedimentation took place in elongated depocenters with oceanward progradation. A second phase of increased sediment supply takes place during the Oligocene and Miocene, resulting in the development of large basinward prograding sedimentary wedges. This event seems to be associated to the interaction between continental dynamics, subsidence, and increased continental erosion during climate shift from greenhouse to icehouse conditions.

Keywords: Colorado Basin, Passive margin, Offshore Argentina, Depocenter migration, Sedimentation rates, South Atlantic

1. Introduction

The Argentine Colorado Basin is one of the major sedimentary basins in the South Atlantic. It is located on the eastern South-American passive continental margin (Fig. 1), where a complex set of sedimentary basins exist in the coastal and inner shelf area.

Passive continental margins are dynamic environments characterised by shallow shelf areas containing thick sedimentary packages derived from onshore erosion. They are therefore an ideal recorder of sedimentary depositional evolution and of the geological development in general. Although passive margin settings are considered to be the result of the transition from a rift phase to drift phase, most passive margins have undergone a complex deformation history. Such deformations are described as a result of salt mobility, margin instability, post breakup flank uplift, and localized compressional deformation (e.g. Brown et al., 2004; Fort et al., 2004; Hudec and Jackson, 2002, 2004; Rowan et al., 2004). Despite the widespread occurrence of strata distribution in most passive margins, few examples exist where there is a good preservation of the entire depositional sequence and its geometry.

The Colorado basin records the deposition of the entire syn-rift and post-rift successions, with a clear tectono-stratigraphic history owing to the apparent absence of salt deposition as well as minimal uplift and erosion. Therefore it is ideally suited to reconstruct the depositional geometry evolution throughout the entire development of a passive margin.

2. Geological and tectonic setting

The Argentine passive margin is mainly of the volcanic rifted type resulting from the break-up of Gondwana and the northward-propagating opening of the South Atlantic (Gladczenko *et al.*, 1997; Hinz *et al.*, 1999; Rabinowitz and Labreque, 1979; Sibuet *et al.*, 1984; Uchupi, 1989; Uliana and Biddle, 1987; Uliana *et al.*, 1989; Franke et al., 2007; 2010). The Colorado Basin records the development of the Lower Cretaceous to present-day volcanic-rifted passive margin of Argentina. After a Permian pre-rift period, the formation of the Colorado Basin is related to the break-up of Gondwana, starting with the rift systems from Triassic/Jurassic (?) to Early Cretaceous, followed by a drift phase and thermal subsidence period through the Cretaceous and ultimately reaching the present-day passive margin configuration of the basin.

The number of extensional phases affecting the continental shelf before the final Late Jurassic – Early Cretaceous phase of the Atlantic extension is still under discussion. Keeley and Light (1993) suggested two phases of active rifting in the Late Triassic-Early Jurassic and in the Mid-Jurassic. The continental extension may have begun in isolated centres in South America

during the Late Triassic/Early Jurassic and almost all of south and west Gondwana was affected by magmatism resulting in a high heat flow (Macdonald *et al.*, 2003). Early Jurassic intraplate extension reactivated pre-existing depocenters and originated new ones such as the San Jorge Basin (Fitzgerald *et al.*, 1990). This early extensional phase may be reflected by the lower syn-rift succession in the North Malvinas Graben (Richards & Fannin, 1997). The major Late Jurassic – Early Cretaceous crustal stretching episode is found throughout the sedimentary basins of the Argentine continental shelf (Keeley and Light, 1993).

One of the early rift phases (either Late Triassic-Early Jurassic, Middle Jurassic or Late Jurassic-Early Cretaceous) was likely oblique and resulted in basins oriented at high angle with respect to the trend of the continent-ocean boundary (Franke *et al.*, 2006; MacDonald *et al.*, 2003). The final opening took place in the Early Cretaceous with proposed ages ranging from 127.7 to 135.5 Ma (Lawver *et al.*, 1998; Nürnberg and Müller, 1991; Rabinowitz and Labreque, 1979). Therefore, sediments within the basin represent the entire sedimentary record from the Late Jurassic rifting of Gondwana (and possibly pre-rift sediments) through the Cretaceous rift and drift episodes until the present day (Fig. 2).

The basement is made up of Precambrian igneous and metamorphic rocks. A blanket of glacial poorly or non-sorted conglomerate or breccia deposited in Late Carboniferous–Early Permian time over most of Gondwana (Macdonald *et al.*, 2003) is preserved in the area of the Colorado Basin (Keeley and Light, 1993). This was covered by dark, organic-rich shales deposited in a major fresh or brackish transgression at the end of the glaciation before a more arid continental environment established in the Triassic (Macdonald *et al.*, 2003). The Permo-Carboniferous sedimentary rocks are exposed as a succession of diamictites, sandstones and dark shales in the La Ventana Hills (Sierras Australes) (Fig. 1b) (Lopez-Gamundi and Rossello, 1998). The succession shows consistent affinity to the Great Karoo Basin of Southern Africa (Keidel, 1916; Keeley and Light, 1993; Lopez-Gamundi and Rosello, 1997).

The syn-rift stratigraphy of the Colorado Basin is speculative as no wells penetrate these sequences. However, sandstones of Early Cretaceous age were drilled in smaller flanking fault blocks that may be equivalents of the depositional infill of the east-west to NW-SE trending grabens and half grabens (Figs. 2 & 3) (Bushnell *et al.*, 2000). Strong and continuous reflectors may additionally indicate lacustrine syn-rift shales of (?)Jurassic and Early Cretaceous age (Fig.2). In the Cruz del Sur well a mix of sandstones with andesites and tuffs was drilled in the syn-rift interval (Bushnell *et al.*, 2000). The Cretaceous Colorado and Fortin Fms. (Albian to Campanian) are dominated by coarse continental to shallow marine

sandstones and conglomerates (Bushnell *et al.*, 2000) but as their lithological content is highly variable the distinction between these two formations is difficult (Fryklund *et al.*, 1996); thus they are jointly referred to the Colorado Fm. in this study. The successions above the Cretaceous sandstones were deposited in a more marine environment and consist mainly of bathyal siltstones and claystones of Upper Maastrichtian to Miocene age (Bushnell *et al.*, 2000). Palaeocene basalts were encountered within the Pedro Luro Fm. (Lesta *et al.*, 1978) at the southern centre part of the basin, evidenced by drilled wells. The Tertiary Facies distribution shows a transition from fluvial-deltaic and shallow marine environment to a deeper marine environment towards the shelf edge (Fryklund *et al.*, 1996; Bushnell *et al.*, 2000).

3. Data set and methodology

The study area covers approximately 95.000 km^2. Using a dense 2D seismic reflection dataset (about 30.000 km) and data from 8 exploration wells (Fig. 1b) provided by Petrobras Argentina and the Federal Institute of Georesources Germany (BGR), we reconstructed the geological evolution of the Colorado Basin. The 2D seismic lines consisted of processed standard industrial reflection seismic lines (post-stack time-migrated). The grid spacing varies from 2.5 to 35 km and the seismic signal reached down to 12.000 ms in two-way-travel time (twt). In addition to the seismic data, some stratigraphic well tops and lithological/biostratigraphic data, as well as checkshots were also provided by Petrobras. Stacking velocities used in time depth conversion were provided by the BGR. Interpretation and time-depth conversion were performed with Petrel™ Interpretation Software (Schlumberger) version 2009.

Seismic-to-well log correlations and integration with biostratigraphic data were carried out in order to provide a chrono-stratigraphic framework for the interpreted surfaces, as well as a detailed seismo-stratigraphic interpretation and tectono-stratigraphic analysis of the basin. Following seismic interpretation of the main reflectors in the study area, a velocity model to convert twt interpreted horizons into depth was defined. The time-depth relation from checkshot data of the individual wells (Fig. 4a) and the stacking velocities from the BGR-lines were used to calculate the interval velocities for the defined seismic units (Fig. 4b). Stacking velocities were determined from analysis of normal move-out measurements from common depth point gather of seismic data. The interval velocity, typically P-wave velocity, of a specific layer of rock was calculated from the change in stacking velocity between

seismic events on a common midpoint gather. Using the interval velocity from 6 wells and from the Dix-conversion of stacking velocity of 3 seismic lines, a final velocity model was elaborated, allowing the conversion from the interpreted twt seismic horizons into true-vertical depth (tvd). By validating the well tops to the depth-converted seismic dataset a uncertainty of ±5% can be estimated. Finally, depth and thickness maps were created from the interpreted sections. Using these maps the volume of each seismic unit was derived and sediment accumulation as well as sedimentation rates were calculated. In addition to the seismic horizons, the major bounding fault systems were mapped on the 2D seismic sections.

4. Results

4.1 Seismo-stratigraphic units

As a result of seismic-to-well log correlations and the integration of biostratigraphic well tops the major syn- and post-rift seismic sequences and their bounding surfaces, such as unconformities and regional seismic markers, were identified and mapped. Furthermore as a result of seismo-stratigraphic interpretation and tectono-stratigraphic analysis the top pre-rift and the break-up unconformity were identified and mapped throughout the basin. The main seismic units identified in the Colorado Basin are shown in Figures 2 and 3. Overlying the pre-rift sequences the Cretaceous succession was subdivided into four seismic units. The syn-rift sediments (?Jurassic/Early Cretaceous) beneath the break-up unconformity were deposited in graben and half-graben systems within the main depocenters of the basin. The post-rift sediments starting with the Sag II and Sag I units (Barremian to Aptian), as well as the Colorado Fm. (Albian to Maastrichtian) were deposited during the basin sag-phase and thicken above the depocenters of the basin. Four Tertiary units were distinguished: the Pedro Luro Fm. (Paleocene), the Elvira Fm. (Eocene), the Caotico informal unit (Oligocene), and the Baranca Final Fm. (Miocene). These sequences are present on the continental shelf and slope region with water depths ranging from 50 to 2250 m (Fig. 1b).

4.2 Main structures

Several structural elements have been analysed by mapping the major bounding faults that can be traced through the Colorado Basin. These faults include:

(1) Rift-related faults resulting in graben and half-graben systems beneath the break-up unconformity. These extensional faults are rooted in the deep pre-rift successions and generally terminate within the syn-rift successions, although some extent into the Lower

Cretaceous (Fig. 3 & 5). The normal faults control the geometry of the main syn-rift depocenters (Fig. 5)

(2) Seismic data shows that the basin was subject to an extensional episode post-dating the formation of the South Atlantic, reactivating the rift-related normal faults during the Cretaceous. These reactivated structures were later capped by Tertiary sediments (i.e. Baranca Final Fm.) (Fig. 6). The reactivated structural elements are commonly found in conjunction with and above the rift faults and do not show any evidence of structural inversion or compression.

(3) The Upper Cretaceous and Lower Tertiary sequences are dissected by a second generation of post-rift normal faults affecting the depositional units of the Colorado and Pedro Luro Fms. (Fig. 7). A semi vertically-faulted interval with dense fault spacing has been identified within these formations in the distal slope area of the basin. These faults are likely to have been generated by slope gravitational tectonics..

We built up four regional profiles accross the Colorado Basin (Fig. 8). They depict clearly present-day basin structure and the main seismo-stratigraphic units identified, including the locations of main depocenters and the relationship between the rift faults and the syn-rift and post-rift units. The NE-SW Profile 1 at the slope area of the basin shows inferred pockmarks, submarine channels, and thick, up to 7800 m accumulations of syn-rift and post-rift sediments up to the top of the Colorado Fm. The main depocenter is dissected by the rift-controlled faults and the Cretaceous extensional-reactivation of these faults is illustrated above the smaller depocenter located in the south-west area. Profile 2 shows a cross-section in N-S direction across the central part of the basin, depicting the onlaps of the Cretaceous and Tertiary successions onto the pre-rift structures. In this profile rift-controlled faults show no signs of reactivation, but result in a high amount of syn-rift grabens and half-grabens, which also controlled the location of the overlying sag-phase depocenters. Profile 3, across the eastern part of the basin, shows a series of grabens and half-grabens, controlled by rift-related faults on both sides. The grabens are filled with thick successions of syn-rift and post-rift sediments and to the south-west the rift faults have been reactivated. Profile 4 displays the entire basin in E-W direction, including the slope, the Continental-Oceanic Boundary (COB), and the oceanic domain. The slope area is characterised by relatively high sedimentation rates and the development of basinward prograding sedimentary wedges. The COB is confirmed by seaward-dipping-reflectors (SDR's), also described by Hinz *et al.,* (1999) and Franke *et al.,* (2007). The profiles show thick successions of syn-rift sediments and the increasing thickness

of the section between the break-up unconformity and the Colorado unconformity towards the centre. The main depocenters are illustrated by the development of syn-rift sediments and the deposition of the basin's sag phases, where the extensional/rift-related faults occur at the flanks of these depocenters. All profiles show relatively thin sedimentary layers of the Tertiary Pedro Luro, Elvira and Caotico units, however the Upper Tertiary Baranca Final Fm. is a thick sedimentary package with a continuous high sediment supply until present day.

4.3 Surface- and isopach maps

The construction of isochronal (twt) maps provided a 3D spatial visualisation of the stratigraphic relationship and the structures of the identified sequences. The depth-converted surface (Fig. 9-i), and isopach (Fig. 10a-h) maps display the evolution of the sedimentary basin infill through time. We observe a clear change in configuration from the break-up unconformity (127.7 to 135.5 Ma) to present-day. In its present-day configuration, the basin is shallower (infill of up to 2000 m) in its flanks, and deepens towards the centre (16,000 m of sediment infill / Fig. 9a). The syn-rift depocenters are comparatively limited in size and contain up to 5500 m of sediments (Fig. 10a). Within the syn-rift sediments, the presence Jurassic and Early Cretaceous organic-rich source rock intervals have been suggested (Fig. 2). The basin sag phase is represented by the sequences deposited between the break-up unconformity (Barremian/Fig. 9b) and the Colorado unconformity (Campanian/Fig. 9e). These Cretaceous successions (Sag II, Sag I, and Colorado Fm.) contain a maximum of 6500 m sediments (Fig. 10b, 10c, and 10e) and onlap on the pre-rift structures in the southern and northern part of the basin (Fig. 9d and 9f). The depth maps of the Sag I and the Colorado Fm. (Figs. 9d and 9e) show that the basin deepens and sediments prograde towards the east. The deposition of the seismic unit Sag I coincides with the possible occurrence of potential Aptian source rocks in the basin (Fig. 2). The continued subsidence and resulting accommodation space has been filled by Tertiary units (Pedro Luro, Elvira, Caotico, and Baranca), with up to 4000 m of sediments deposited until the end of the Miocene (Fig. 10e, 10f, 10g, and 10h). The Pedro Luro Fm. marks the Cretaceous/Tertiary boundary in the sedimentary succession (Fig. 9f). The Pedro Luro, Elvira and Caotico units onlap onto the pre-rift structures towards the north and south (Fig. 10e and 10f, and 10g). The Baranca Final Fm. (Miocene) and the Belen Fm. (Pleistocene) concludes the history of basin filling (Fig. 10h).

4.4 Depocenter migration and stratigraphic evolution

As mentioned, the pre-rift successions are dissected by numerous extensional faults, resulting in the formation of graben and half-graben systems in the basin, controlling the location of the syn-rift depocenters (Fig. 5). The pre-rift deposits appear as mainly parallel seismic reflectors, both at the base of the graben structures and at the horsts (Figure 11). It is suggested from well data, that this succession represents Late Carboniferous–Early Permian conglomerate or breccia and finer lithologies (Macdonald *et al.*, 2003; Keeley and Light, 1993). The pre-rift succession displays a central EW-elongated graben which influences thicknesses in the overlying sequences up to the Miocene. To the East, the E-W Colorado Basin turns NW-SE, becoming perpendicular to the present-day continental margin (oriented NE-SW).

Three major syn-rift depocenters were identified in the basin with a maximum thickness of 5500 m within one of the main depocenter (Fig. 10a). Beneath the break-up unconformity, the syn-rift sediments are predominantly present in NW-SE trending depocenters. The break-up unconformity appears as an erosional surface along the shelf and forms the base of the post-rift sediments in the basin. The pre-rift unconformity is characterized by erosional truncation of the pre-rift strata in the grabens and the syn-rift sequence (or sequences) shows onlap onto the pre-rift unconformity. Above the break-up unconformity the post-rift sediments starting with the thickness of the Sag II phase and the main depocenters are located in the centre of the basin trending in an E-W direction (Fig. 10b). During the Sag I phase deposition of these successions was confined to the centre-west and to the south-east parts of the basin (Fig 10c), maintaining the NW-SE and E-W trend. The thickness map of the Colorado Fm. (Albian - Maastrichtian) displays a thickening of the sediments in the eastern centre part of the basin and its depocenter turns NW-SE towards the East (Fig. 10d).

From this time onward, a NE-SW trending shelf break developed with progradation and concurrent activity of mass movement of the sediments of the Colorado Fm. (Fig. 10d, 10e and Fig. 12b). Seismic data shows that the basin was subject to an extensional episode postdating the formation of the South Atlantic, reactivating the rift-related normal faults during the Cretaceous. The post-rift sequences of the Cretaceous deposits vary from less than 500 m to 6500 m and from the Aptian to Maastrichtian shelf progradation to the east dominated. The Colorado Fm. (Albian-Maastrichtian) is characterized by fairly parallel bedding and close to the continental slope its top is marked by an erosional unconformity. The top-Maastrichtian erosional unconformity was transgressed by the Paleogene (Paleocene–Eocene) sequences. The Tertiary units, starting with the Pedro Luro Fm. (Paleocene), are up

to 4000 m thick and during the Paleocene to Oligocene aggradation prevailed in the centre of the basin. The Tertiary successions are characterized by parallel reflectors, indicating that they were deposited during a tectonically quiescent period. There is no evidence for erosions larger than a few tens of meters after the break-up unconformity. Throughout the deposition of the Pedro Luro Fm. (Paleocene) the depocenter is concentrated at the slope of the basin (Fig. 10e), probably as a result of progradation towards the shelf edge. During the deposition of the Elvira Fm. (Eocene) the depocenters migrated back towards the centre and western area of the basin (Fig. 10f) where aggradation became dominant and sediment thickness decreased. The Late Tertiary depocenter is mainly concentrated in the eastern part of the basin as documented by the deposition of the Caotico and Baranca/Belen units (Fig. 10g and 10 h). The Tertiary successions are more or less parallel layered in the centre part of the basin suggesting sediment aggradation during this time. Whilst from the Oligocene to the Miocene sediment deposition increased and relatively high sedimentation rates continued to the present day with the development of basinward prograding sedimentary wedges. The Cretaceous and Tertiary units onlap onto the pre-rift structures in the north and south of the basin (Fig. 12a). The Upper Cretaceous and Lower Tertiary sequences are dissected by a second generation of post-rift normal faults affecting the depositional units of the Colorado and Pedro Luro Fms. (Fig. 7) at the slope of the basin, resulting from gravitational tectonics and slumping episodes. In summary, from the Aptian to Maastrichtian, shelf progradation dominated whilst during the Paleocene to Oligocene, aggradation prevailed. During the Eocene sediment deposition decreased, related to limited available accommodation space (Table 1). From the Oligocene to the Miocene sediment deposition increased due to higher available accommodation space and relatively high sedimentation rates continued to the present day with the development of basinward prograding sedimentary wedges.

4.5 Sedimentation rates

, The sedimentation rates for each unit were derived by calculating volumetric accumulation rates over time and averaging these over the area of deposition (Table 1). The sedimentation rates are independent measures of sedimentation in meters per million years (Ma). Assuming an accumulation time span of 25 My for the syn-rift successions, sedimentation rates of 118 m/My are estimated (Table 1, Fig. 13). The accumulations in this period most likely represent a dominantly continental environment with siliciclastic lacustrine sediment infill and volcanics. By Late Cretaceous post-rift thermal subsidence dominated the basin development. During the early phase of subsidence, high sedimentation rates of up to 122 m/My occurred in

the basins sag-phase, which was mainly restricted to the structural geometry of the rift basin. During the deposition of the Colorado Fm. (Albian to Maastrichtian), with coarse continental to shallow marine sandstones and conglomerates, sedimentation rates decrease dramatically to 30 m/My. During this period (44 Ma) the bulk of the sediment were deposited by progradation to the east of the basin, whilst throughout the Late Cretaceous sedimentation took place in elongated depocenters with oceanward progradation. A second phase was related to thermal subsidence along the trend of the South Atlantic margin throughout the Tertiary (Fig. 13). During this time, the basin developed under truly marine conditions and sedimentation rates are relatively high (47 m/Ma) in the Paleocene, when the section becomes marine for the first time. The sediments consist mainly of bathyal siltstones and claystones. This major Paleocene marine transgression was followed by a period of uplift of South America that triggered a regression and low sedimentation rates (12 m/Ma) during Elvira Fm's deposition (Eocene), which is a condensed section characterised by shales deposition . The Late Paleogene-Neogene facies distribution shows a transition from shallow marine and fluvial-deltaic environment to a deeper marine environment towards the shelf edge and relatively high sedimentation rates (54 m/Ma) are calculated during Oligocene time and remained high (40 m/Ma) until the end of Miocene. These relatively high sedimentation rates continued until the present day with the development of large basinward-prograding sedimentary wedges. This increase in sedimentation rates correlates with the global climatic transition from greenhouse to icehouse conditions (Fig. 13), which is thought to have influenced the enhancement of continental erosion (Seranne 1999, Anka and Seranne 2004). In addition, subsidence was still ongoing creating the necessary accommodation space during this time and both aggradations within the central part of the basin, as well as progradation towards the east took place.

5. Discussion

5.1 Basin evolution and comparison with conjugate margin

This This study shows that the Colorado Basin initially evolved in an NW-SE trending direction during pre-rift/early syn-rift and changed to a E-W trending direction during the Sag II phase. The direction of extension changed again to NE-SW towards the East during early basin formation, and shifted to a NW-SE direction of extension during the Late Cretaceous along the Atlantic margin, corresponding to the opening direction of the South Atlantic. Franke et al. (2006) conclude that the basin is mainly an extensional basin and not an

intracontinental sag basin, which coincides with our observations. The strong obliquity of the basin with respect to the South Atlantic opening direction (NE-SW) could be explained by assuming t that the Colorado Basin represents a failed rift which developed in early stages of the South Atlantic formation, whereby the two other arms of the tripartite system have formed the main Atlantic spreading centre. However, this study confirms that the origin of the NW-SE oblique rift most probably resulted from extensional stress, either acting through or interacting with the prevailing Palaeozoic basement fabric, which coincides with the observations from Franke at al. (2006). Hence, we suggest that the geometry and structure of the inherited part of the Colorado Basin represents an earlier rift phase pre-dating the main break-up of the South Atlantic, which could be related to pull-apart basins formation. Such pull-apart basins have been proposed in the South Atlantic offshore and onshore Argentina (Franke *et al.,* 2006; Tankard *et al.,* 1995; Uliana *et al.,* 1989; Uliana and Biddle, 1987), as well as in the foreland basins of southernmost South America (Ghiglione *et al.,* 2010; Uliana, et al 1989). The Colorado Basin still may be a failed rift; however, we propose that pre-rift inheritance (Fig. 11) was the main control for the direction of the NW-SE segment of the basin (Fig. 5, 6 and Fig. 8/Profile 1). We do not have a conclusive timing regarding the initiation of the basin, but the large dimensions of the syn-rift graben structure - extending up to 30 km in width- (Fig. 10a, suggest that rifting took place earlier than the final rift phase (156 Ma) that resulted in the break-up of the South Atlantic. The well penetration of basalts within the Paleocene (Pedro Luro Fm.) does not support the existence of another late rifting phase as these mapped volcanic areas do not correspond to any depocenter.

The evolution of a sedimentary basin depends on the interplay of various factors: the thermal subsidence history, compaction, tectonic uplift, and climatic conditions that affect the style and magnitude of erosion and sedimentation. The interpretation of more than 30,000 km of seismic reflection data of the Colorado Basin has led to a better understanding of the subsidence history during the early rift/drift stages. In the basin tectonic subsidence started with the initial rifting around 156 Ma and it was relatively rapid for approximately 50Ma, before it decreased and continued with a more or less constant rate until today. The Colorado Fm. is interpreted to reflect sedimentation during the thermal subsidence stage, which affected the Argentine continental margin during the first part of the drift phase. Seismic data and well data give no evidence for erosion of more than a few tens of meters after the break-up unconformity.

Although the duration of extensional phases preceding the final break-up of the South Atlantic is unclear, most authors suggest an extensional period of about 25 Ma (Uliana *et al.*, 1989; Harry and Sawyer 1992). Assuming an accumulation time span of 25 Ma for the syn-rift successions, sedimentation rates of 118 m/Ma are estimated (Table 1, Fig. 13). Such high sedimentation rates of syn-rift deposits have so far not been described on the eastern Argentine margin, nor in the conjugated Orange Basin in South Africa. By late Cretaceous, the Gondwana break-up had stopped in almost all areas and post-rift thermotectonic subsidence and minimal faulting dominated the basin development from there on (Vayssaire *et al.*, 2007). This study confirms that the basin underwent two phases of thermal subsidence resulting in distinct variations of the post-rift successions, which also correspond to the observations made by different authors (Galeazzi, 1998; Hinz *et al.*, 1999; Uchupi, 1989; Sibuet *et al.*, 1984) (Fig. 13). During the early phase of subsidence (the sag phase) high sedimentation rates (122 m/Ma) are observed (Sag I and Sag II units; Fig. 13, Table 1). Whereby the first phase was mainly restricted to the structural geometry of the rift basin.

During the deposition of the Colorado Fm. (Albian to Maastrichtian) sedimentation rates decrease dramatically to 30 m/Ma, such local sedimentation rates may not represent the entire system. However, these relatively low sedimentation rates can be explained by low accommodation space above the structural geometry of the rift basin. Throughout the Late Cretaceous (Albian to Maastrichtian) sedimentation took place in elongated depocenters, with the bulk of the sediment being deposited by sediment progradation to the east (oceanward) of the basin. This study shows that thick succession of Cretaceous and Tertiary sediments were deposited at various points along the shelf edge, which also correspond to observations made along the Argentine shelf edge in general (Urien *et al.*, 1981). The second phase was related to thermal subsidence along the trend of the South Atlantic margin during the Tertiary (Fig. 13). During this time, the basin developed under marine conditions and sedimentation rates are relatively high (47 m/Ma) in the Paleocene. Relatively low sedimentation rates (12 m/Ma) occurred during the Eocene (Elvira Fm.) with the deposition of shales. This might be explained by the major marine transgression during the Paleocene, which was followed by a period of uplift of South America during the Eocene (Urien *et al.*, 1981) that triggered a regression of large magnitude resulting in the low sedimentation rates during the deposition of the Elvira Fm. (Eocene). This drop in sedimentation rates might also be the origin of the condensed section of the Elvira Formation. The Late Paleogene/Neogene facies distribution shows a transition from shallow marine and fluvial-deltaic environment to a deeper marine

environment towards the shelf edge and relatively high sedimentation rates (54 m/Ma) are calculated during Oligocene time and remained high (40 m/Ma) until the end of Miocene. This increase in sedimentation rates corresponds to the global climatic transition from greenhouse to icehouse environment (Fig. 13), which had a strong effect on the glaciation of the Andes and resulting glacial erosion. In addition, thermal subsidence was still ongoing, creating the necessary accommodation space during this time and both aggradation within the central part of the basin, as well as progradation towards the east took place until present day. The higher sedimentation rates in the Colorado Basin during the Oligocene and Miocene are in contrast to the low sedimentation rates registered in the southern Orange Basin, in the conjugate margin, during the same period of time, which might be explained by substantial sediment bypass the middle shelf area , although may also be explained by comparably smaller thermal subsidence in the southern Orange Basin (Kuhlmann *et al.*, 2010).

Vayssaire *et al.*, (2007) state that a second extensional episode occurred in the Colorado Basin between 95-80 Ma. This study confirms the reactivation of the main faults during this time interval as seen by the reactivated rift-controlled faults (Fig. 6 & 8). The Upper Cretaceous and Lower Tertiary sequences are dissected by a second generation of post-rift normal faults affecting the depositional units of the Colorado and Pedro Luro Fms, during which the highly vertical faulted interval at the distal slope area was developed (Fig. 7). The migration of depocenters during Mid Cretaceous from the eastern centre to the slope of the basin is related to the progradation towards the shelf break. The progradation took place with minor slumping episodes indicating slope instability associated with gravitational tectonics at the distal slope. These events/structures were later sealed by the Pedro Luro Fm. (Paleocene). From the Upper Cretaceous onwards the continental margin is affected by slope instabilities as seen in the high vertical faulted interval with seaward-dipping normal faults (Fig. 7). The main Cretaceous/Tertiary phases of slope instabilities affected the units of the Colorado and the Pedro Luro Fms. Cretaceous slumps are observed in the eastern part of the Colorado basin which had relatively high sedimentation rates during that time and shows interplay of progradation and slumping (Fig. 12b). It appears that the Upper Tertiary Caotico Unit (Oligocene) and Baranca Final Fm. (Miocene) are relatively undisturbed.

On the conjugate Orange Basin, Kuhlmann *et al.*, (2010) stated that the seaward dipping extensional faults only developed above dipping decollement surfaces of the Upper Cretaceous at the shelf break, similar to the location of the observed Cretaceous slumps in this study (Fig. 7). Another controlling factor for the occurrence and style of the slumping is the

variation in sedimentation rates (Fig. 13). However, paleogeographic conditions during the slumping episodes were different during both time intervals. While Late Cretaceous slumping took place in a relatively narrow proto-South Atlantic, with low discharge rates of the Colorado River (Bushnell *et al.*, 2000; Galeazzi, 1998; Hinz *et al.*, 1999) and decreasing crustal subsidence in the elongated depocenters, the Tertiary mass movements occurred during a time of higher sediment supply and thermal subsidence. Several triggering mechanisms have been postulated as the cause of slope instability and sediment collapse. These include rapid sedimentation rates and resulting high internal pore fluid pressures, as well as down-slope undercutting (Emery *et al.*, 1975; Dingle *et al.*, 1983). This study shows that in the Colorado Basin the slumping episodes are mostly related to the progradation of the sediments, the sediment build up at the slope, and further development of seaward dipping normal faults.

6. Conclusions

The evolution of the Colorado Basin has been interpreted through the detailed analysis of the seismo-stratigraphic sequences identified in the basin and the estimation of the sedmentation rates through time. The syn-rift and post-rift (thermal sag phase) evolution of the Colorado Basin and its geometry is mainly controlled by rift bounding faults, which resulted in the formation of graben and half-graben systems where the main depocenters developed. Three main syn-rift depocenters have been identified, whereby the thickest one contains up to 5.5 km of sediments.

Three faulting events are recognized in the basin: (1) The rift-related faults resulting in graben and half-graben systems, (2) A second extensional episode, which reactivated the rifting normal faults during the Upper Cretaceous and (3) A generation of post-rift normal faults, which affected the Upper Cretaceous and Lower Tertiary sequences (Colorado and Pedro Luro Fms.) in the slope.

Our results confirm that the Colorado Basin is a typical extensional basin which formed in close connection with the development of the South Atlantic. The origin of the NW-SE oblique rift most probably resulted from extensional stresses, either acting through or interacting with the prevailing Palaeozoic basement fabric. Hence, we propose that the geometry and structure of the inherited part of the Colorado Basin represents an earlier rift phase pre-dating the main break-up of the South Atlantic.

The thermal subsidence in the basin started with the initial rifting around 156 Ma ago and it was relatively rapid for approximately 50Ma, before it decreased and continued with a more or less constant rate until today. The Colorado Fm. is interpreted to reflect sedimentation during the thermal subsidence stage, which affected the Argentine continental margin during the drift phase. With an accumulation time span of 25 Ma for the syn-rift succession, which correspond to the duration of extensional phases preceding the final break-up of the South Atlantic, estimated sedimentation rates are of 118 m/Ma. By Late Cretaceous, the Gondwana break-up had stopped in almost all areas and post-rift thermal subsidence dominated the basin development. During the early phase of subsidence (Early Cretaceous), high sedimentation rates of up to 122 m/Ma occurred in the basins sag-phase, which was mainly restricted to the structural geometry of the rift basin. Low sedimentation rates occurred throughout the Late Cretaceous and sedimentation took place in elongated depocenters with oceanward progradation. A second phase of thermal subsidence along the trend of the South Atlantic margin during the Tertiary was concomitant with a drastic increase in sediment supply during the Oligocene and Miocene, resulting in the development of large basinward prograding sedimentary wedges. These high sedimentation rates are associated to continental dynamics, thermotectonic subsidence, and the change from greenhouse to icehouse conditions. From the Cretaceous onwards the continental margin is affected by slumping episodes. The main Cretaceous/Tertiary phases of mass movements affected the Colorado Fm. (Campanian) and the Pedro Luro Fm. (Paleocene). The slumping episodes are related to the progradation of the sediments and the sediment build-up at the slope as well as to the development of the seaward dipping extensional faults.

Acknowledgements

This study was funded by the German Science Foundation (DFG) priority program "SAMPLE" Phase I. Z. Anka's position is funded by a Helmholtz-University Young Investigators Group grant from the Helmholtz Association of German Research Centres. We gratefully acknowledge Petrobras Argentina (PESA) and the German Federal Institute for Geoscience and Natural Resources (BGR) for supplying data and allowing publication of these results. Prof. Eduardo Rosello and an anonymous reviewer are thanked for their insightful comments and suggestions which helped to improve earlier versions of this manuscript.

References

Anka, Z. and Séranne, M., 2004. Reconnaissance study of the ancient Zaire (Congo) deep-sea fan (ZaiAngo Project). Marine Geology (209): 223-244.

Bushnell, D.C., Baldi, J.E., Bettini, F.H., Franzin, H., Kovas, E., Marinelli, R., and Wartenburg, G.J., 2000. Petroleum system analysis of the eastern Colorado Basin, offshore northern Argentina, in Mello, M.R., and Katz, B.J., eds., Petroleum systems of the South Atlantic margins:A.A.P.G. Memoir (73): 403-415.

Dingle, R.V., Siesser, W.G., Newton, A.R., 1983. Mesozoic and Tertiary Geology of southern Africa. A.A. Balkema, Rotterdam, 355 pp.

Emery, K.O., Uchupi, E., Bowin, C., Phillips, J., Simpson, E.S.W., 1975. Continental margin off western Africa: Cape St. Francis (South Africa) to Walvis ridge (Southwest Africa). AAPG Bulletin 59, 3–59.

Franke, D., Neben, S., Schreckenberger, B., Schulze, A., Stiller, M., and Krawczyk, C.M.,2006. Crustal structure across the Colorado Basin, offshore Argentina. Geophys. J.Int.(165): 850–864.

Franke, D., Neben, S., Ladage, B., Schreckenberger, B., Hinz, K., 2007. Margin segmentation and volcano-tectonic architecture along the volcanic margin off Argentina/Uruguay,South Atlantic. Marine Geology, 244, pp. 46-67.

Fryklund, B., Marshal, A. and Stevens, J., 1996. Cuenca del Colorado. In: V.A.T. Ramos,M.A., (Editor), Geologia y recursos naturales de la plataforma continental Argentina,relatario XIII. Congreso Geologico Argentino y III. Congreso de Exploracion de Hidrocarboros,. Associacion Geologica Argentina & Inst. Argentino del Petroleo, Buenos Aires, pp. 135–158.

Galeazzi, J.S., 1998. Structural and stratigraphic evolution of the western Malvinas Basin, Argentina. A.A.P.G. Bull., 82(4): 596-636.

Gladczenko, T.P., Hinz, K., Eldholm, O., Meyer, H., Neben, S., Skogseid, J. (1997). South Atlantic volcanic margins. J. Geol. Soc. London, 154, 465-470.

Ghiglione, M.C., Quinteros, J., Yagupsky, D., Bonillo-Martínez, P., Hlebszevtich, J., Ramos, V.A., Vergani, G., Figueroa, D., Quesada, S., Zapata, T., 2010. Structure and tectonic history of the foreland basins of southernmost South America. Journal of South American Earth Sciences. Elsevier, 29, 262-277.

Granjeon, D. and Joseph, P., 1999. Concepts and applications of a 3D multiple lithology, diffuse model in stratigraphic medelling, in Harbough J.W. & al., eds., Numerical experiments in stratigraphy, SEPM Sp. Pub. 62.

Harry, D.L., Sawyer, D.S., 1992. Basaltic volcanism, mantle plumes and the mechanics of rifting: the Parana flood basalt province of South America, *Geology,* **20,** 207–210.

Haskell, N., Grindhaug, J., Dhanani, S., Heath, R., Kantorowicz, J., Antrim, L., Cubanski,M.,Nataraj, R., Schilly,M.,Wigger, S., 1999. Delineation of geological drilling hazards using 3-D seismic attributes. Lead. Edge 373–382 (March 1999).

Hinz, K., Neben, S., Schreckenberger, B., Roeser, H.A., Block, M., Goncalves de Souza, K., and Meyer, H., 1999. The Argentine continental margin north of 48°S: sedimentary successions, volcanic activity during break-up. Mar. & Petrol. Geol.(16): 1-25.

Jacquin, T. and de Graciansky, P.C.H., 1988. Cyclic fluctuations of anoxia during Cretaceous time in the South Atlantic Ocean. Mar. & Petrol. Geol.(5): 359–369.

Juan, R. del C., De Jager, J., Russell, J. & Gebhard, I., 1996. Flanco norte de la cuenca delColorado, in Geologia y recursos naturales de la plataforma continental Argentina,relatario XIII◦ Congreso Geologico Argentino y III◦ Congreso de Exploracion deHidrocarboros, pp. 117–134, eds Ramos, V.A. & Turic, M.A., Association Geologica Argentina & Inst. Argentino del Petroleo, Buenos Aires, Argentina.

Katz, J. and Mello, M., 2000. Petroleum system of South Atlantic Marginal basins – An overview. A.A.P.G. Memoir(73): 1-13.

Keeley, M.L. and Light, M.P.R., 1993. Basin evolution and prospectivity of the Argentine continental margin. J. Pet. Geol., 16(4): 451-464.

Keidel, J., 1916. La geologia de las sierras de la provincia de Buenos Aires y sus relaciones con las montañas de Sudàfrica y los Andes. Ministerio de Agricultura, Secciòn Geologia, Buenos Aires, Anales 11 (3).

Kopf, A., 2002. Significance of mud volcanism. Reviews of Geophysics 40 (2), 1–52.

Lawver, L.A., Gahagan, L.M. and Dalziel, I.W.D., 1998. A tight fit – Early Mesozoic Gondwana, a plate reconstruction perspective. Polar. Res.(53): 214–229.

Lesta, P.J., Turic, M.A., Mainardi, E., 1978. Actualization de la information estratigrafica en la Cuenca del Colorado, VII° Congresso Geologico Argentino (Neuquen, 1978), Actas I, pp. 701-713, Buenos Aires.

Lopez Gamundi, O.R., and Rossello, E.A., 1998. Basin fill evolution and paleotectonic patterns along the Samfrau geosyncline: the Sauce Grande basin-Ventana foldbelt (Argentina) and Karoo basin-Cape foldbelt (South Africa) revisited. Geol. Rundsch., 86:819-834.

Macdonald, D. Gomez-Perez, I., Franzese, J., Spalletti, L., Lawver, L., Gahagan, L., Dalziel, I., Thomas, C., Trewin, N., Hole, M., and Paton, D., 2003. Mesozoic break-up of SW Gondwana: implications for regional hydrocarbon potential of the southern South Atlantic. Marine and Petroleum Geology. 20(3-4): 287-308.

Mancilla, O., Salinas, A., Soubies, D., Debarre, R. and Granjeon, D., 2001. Numerical stratigraphic modeling of the offshore Colorado Basin of Argentina: Methology and results, AAPG Hedberg Conference.

Mancilla, O., Salinas, A., Soubies, D., Debarre, R. and Granjeon, D., 2002. Exploración en Aguas Profundas en la Cuenca del Colorado, República Argentina. Utilización del modelado estratigráfico numérico, V Congreso de Exploración y Desarrollo de Hidrocarburos, Buenos Aires, pp. 19 pp.

Nürnberg, D. and Müller, R.D., 1991. The tectonic evolution of the South Alantic from Late Jurassic to Present. Tectonophysics, 191: 27-53.

Rabinowitz, P.D. and Labreque, J., 1979. The Mesozoic South Atlantic Ocean and evolution of its continental margins. J. Geophys. Res., 84(B11): 5973-6003.

Richards, P.C. and Fannin, N.G.T., 1997. Geology of the North Falkland Basin. Journ. Petrol. Geol., 20, 165-183.

Richards, P., Duncan, I., Phipps, C., Pickering, G., Grzywacs, J., Hoult, R., and Merritt, J., 2006. Exploring for fan delta sandstones in the offshore Falklands basins. J. Pet. Geol., 29(3): 199-214.

Rodriguez, J.F., Miller, M. and Cagnolatti, M.J., 2008. Sistemas Petroleros de Cuenca Austral, Argentina, Chile, Instituto Argentino del Petróleo y del Gas, PP. 1-31.

Schümann, T.K., 2002. The hydrocarbon potential of the deep offshore along the Argentine volcanic rifted margin. Ph.D. Thesis, RWTH Aachen, 194 pp.

Séranne, M., 1999. Early Oligocene stratigraphic turnover on West Africa continental margin: a signature of the Tertiary greenhouse to icehouse transition? Terra Nova 11, 135–140.

Sibuet, J.-C. et al., 1984. Early evolution of the South Atlantic ocean: Role of the rifting episode. In: W.W. Hay and J.-C. Sibuet (Editors), Initial reports of the Deep Sea Drilling project, pp. 469-481.
Stoakes, F.A., Campbell, C.V., Cass, R., Ucha, N., 1991. Seismic stratigraphic analysis of the Punta del este basin, offshore Uruguay. South America. Bull. AAPG, 75, 219-240.

Stuevold, L. M., R. B. Faerseth, L. Arnesen, J. Cartwright, and N. Moller, 2003, Polygonal faults in the Ormen Lange Field, More Basin, offshore Mid Norway, in P. van Rensbergen, R. Hillis, A.-J. Maltman, and C.-K. Morley, eds., Subsurface sediment mobilization, v. 216: London, United Kingdom, Geological Society of London, p. 263-281.

Tankard, A.J. et al., 1995. Structural and Tectonic Controls of Basin Evolution in Southwestern Gondwana During the Phenerozoic, in Petroleum Basins of South America, pp. 5–52, eds Tankard, A.J., Su´arez Soruco, R. & Welsink, H.J., Am. Assoc. Petrol. Geol. Mem., 62, USA.

Uchupi, E., 1989. The tectonic style of the Atlantic Mesozoic rift system. Journal of African Earth Sciences, 8: 143-164.

Uliana, M.A. and Biddle, K.T., 1987. Permian to Late Cenozoic evolution of Patagonia, main tectonic events, magmatic activity, and depositionaltrends. In: G.D. McKenzie (Editor), Gondwana six: structure, tectonics, and geophysics,. AGU, Washington, DC.

Uliana, M.A., Biddle, K.T. and Cerdan, J., 1989. South Atlantic fits and intraplate boundaries in Africa and South America,. Tectonophysics (155.): 169–179.

Uliana, M. A., Biddle, K. T., and Cerdan, J. (1989). Mesozoic extension and formation of Argentine sedimentary basins. In A. J. Tankard and H. R. Balkwill (Eds.) Extensional tectonics and stratigraphy of the North Atlantic margins Vol. 46 (pp. 599–614). AAPG Mem.

Unternehr, P., Curie, D., Olivet, J.-L., Goslin, J. and Beuzart, P., 1988. South Atlantic fits and intraplate boundaries in Africa ans South America. Tectonophysics(155): 169-179.

Urien, C.M., Zambrano, J.J. and Martins, L.R., 1981. The basins of southeastern South America (southern Brazil, Uruguay, and eastern Argentina), including the Malvinas Plateau and southern South Atlantic paleogeographic evolution,. In: W.M. Volkheimer, E.A. (Editor), Cuencas sedimentarias del Jurasico y Cretacico en America del Sur. Comite Sudamericano del Jurasico y Cretacico, pp. 45–126.

Vayssaire, A., Prayitno, W., Figueroa, D. and Quesada, S., 2007. Petroleum systems of Colorado and Malvinas basins, deep water Argentina, South Atlantic petroleum systems. Geol. Soc. London, London, pp. 10.

Figure captions:

Figure 1. (a) Location of the Colorado Basin in the South Atlantic, offshore Argentina (red rectangle) and the location of the Orange Basin, offshore South Africa (white rectangle). (b) 2D seismic grid of the Colorado Basin with 2D bathymetry and borehole locations (white dots) used in this study. Profiles 1-4 correspond to the highlighted surveys in Figure 8.

Figure 2. Chronostratigraphic and sequence stratigraphic chart for the Colorado Basin including seismic horizons mapped within this study. In addition, the different elements of potential petroleum systems are specified (Modified after Vayssaire et al., 2007).

Figure 3. Major seismic units identified in the Colorado Basin. These sequences were mapped through the basin.

Figure 4. (a) Depth to TWT plot showing the velocities of used wells. (b) Spatial distribution of velocities, exemplary of top pre-rift, including locations of used well velocities (white dots) and the dotted blue line represent available stacking velocities in the study area. This unit that has the best data coverage shows a distinct increase towards the main depocenter location.

Figure 5. Rift-related faults along the margin of the Colorado Basin. These extensional faults are rooted in the deep basement, including pre-rift sediments, and generally terminate within the syn-rift successions, although some may extent within the Lower Cretaceous.

Figure 6. Basement-controlled faults beneath the break-up unconformity and evidences of a second extensional episode, which reactivated the rifting normal faults (white arrows).

Figure 7. A highly-faulted interval within the Colorado (Campanian) and Pedro Luro (Paleocene) Fms. at the distal slope region of the basin. High-amplitude reflectors within the upper part of the Colorado Fm., between the Tertiary/Cretaceous bounding faults, suggest gas accumulation in these levels.

Figure 8. Regional TWT profiles showing the main seismo-stratigraphic units and structures identified in the Colorado Basin, including the locations of main depocentres and how the basement faulting affects the upper sequences. Profile 4 shows the entire basin in E-W direction, including the slope and the location of the Continental-Ocean-Boundary (COB). See locations in Figure 1b.

Figure 9a-i. Depth-converted maps depicting the structure of the main syn-rift (Permian/Jurassic/Early Cretaceous) and post-rift (Cretaceous/Tertiary) units identified in the basin.

Figure 10a-h. Isopach maps depicting the main depocenters of the main identified units in the basin.

Figure 11. Seismic parallel reflectors at the base of the graben structures characterize the pre-rift deposits. The syn-rift sequences show onlap onto the top of the pre-rift unconformity.

Figure 12. (a) Seismic section in south to north direction, showing the onlaps of Cretaceous and Tertiary units onto the pre-rift structures in the northern part of the basin. (b) Seismic section at the slope of the basin, showing progradation and Cretaceous slumps.

Figure 13. Comparison of accumulation and sedimentation rates for the Colorado Basin at the Argentine margin, western South Atlantic and the southern Orange Basin at the western South African margin, eastern South Atlantic, together with the tectonic development of the eastern margin and global climate proxies. The blue arrows indicate main phases of erosion as observed in the study area and the green arrows indicate phases of fault activity. SR = source rock.

Table 1. Estimation of total deposited area and volume as well as accumulation and sedimentation rates for the units identified in the Colorado Basin.

Table 1

Click here to download high resolution image

Units	Age [Ma]	Sum Volume [km^3]	Sum Duration [Ma]	Accumulation Rate [$km^3/max10^3$]	Area of Deposition [km^2]	Sedimentation Rate [m/Ma]
Baranca	25	137000	25	5,48	160837	40
Caotico	34	49000	9	5,4	160685	54
Elvira	56	26200	22	1,19	160495	12
Pedro Luro	66	28200	10	2,82	160143	47
Colorado	110	120000	44	2,72	160007	30
Sag I + II	130	121800	20	6,09	159929	122
Syn-rift	155	152000	25	6,08	159743	118

Figure 1

Click here to download high resolution image

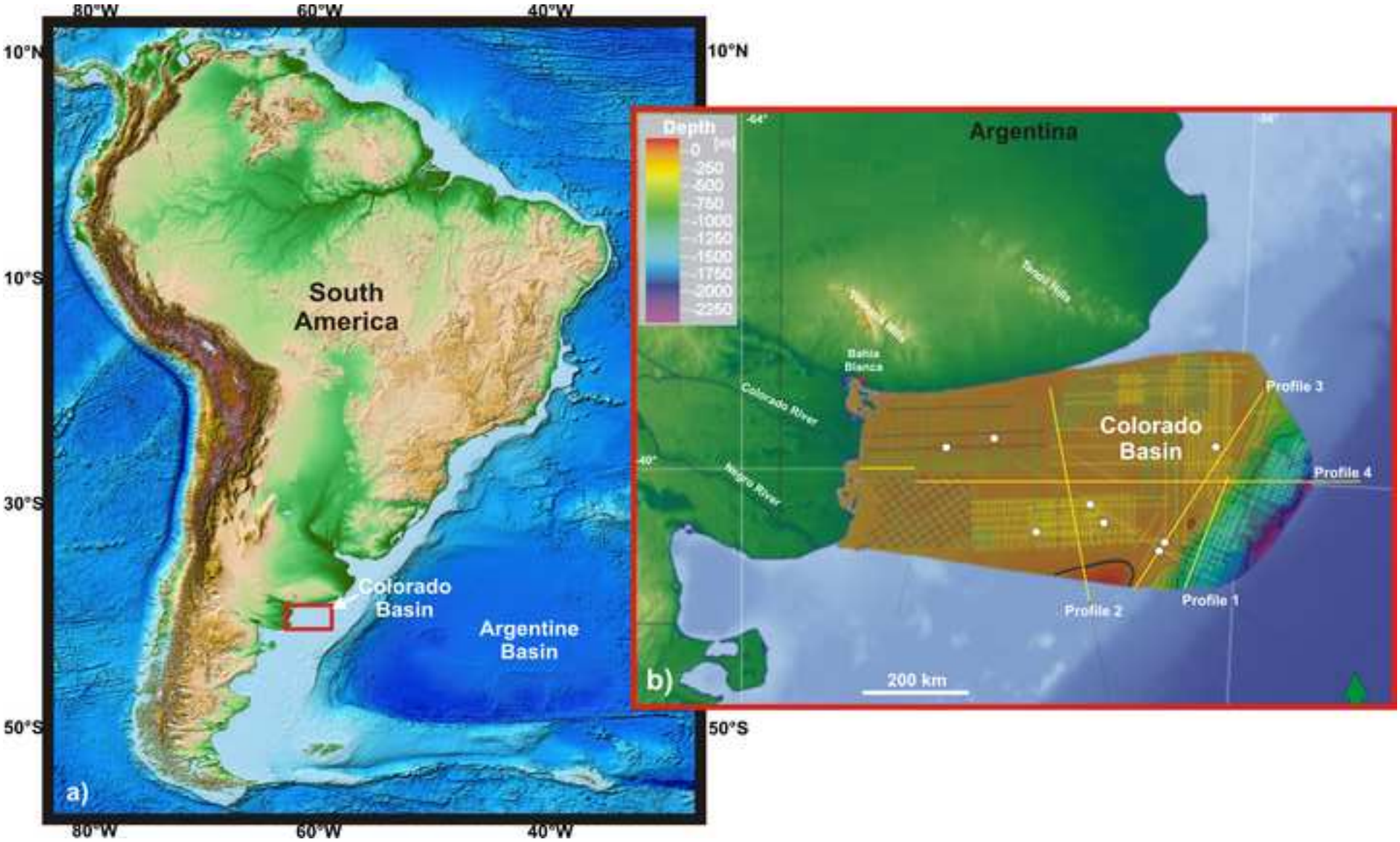

Figure 2

Click here to download high resolution image

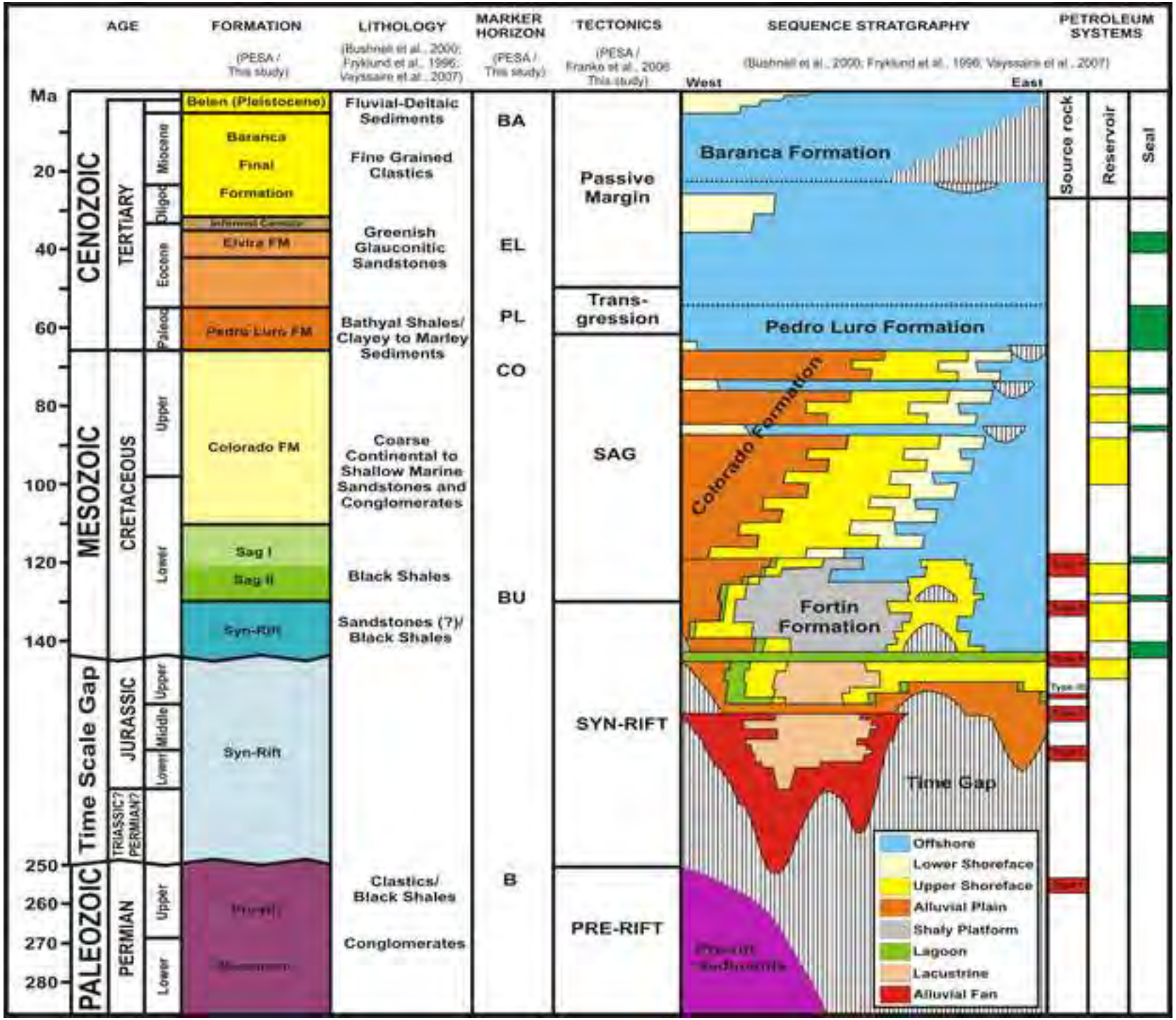

Figure 3

Click here to download high resolution image

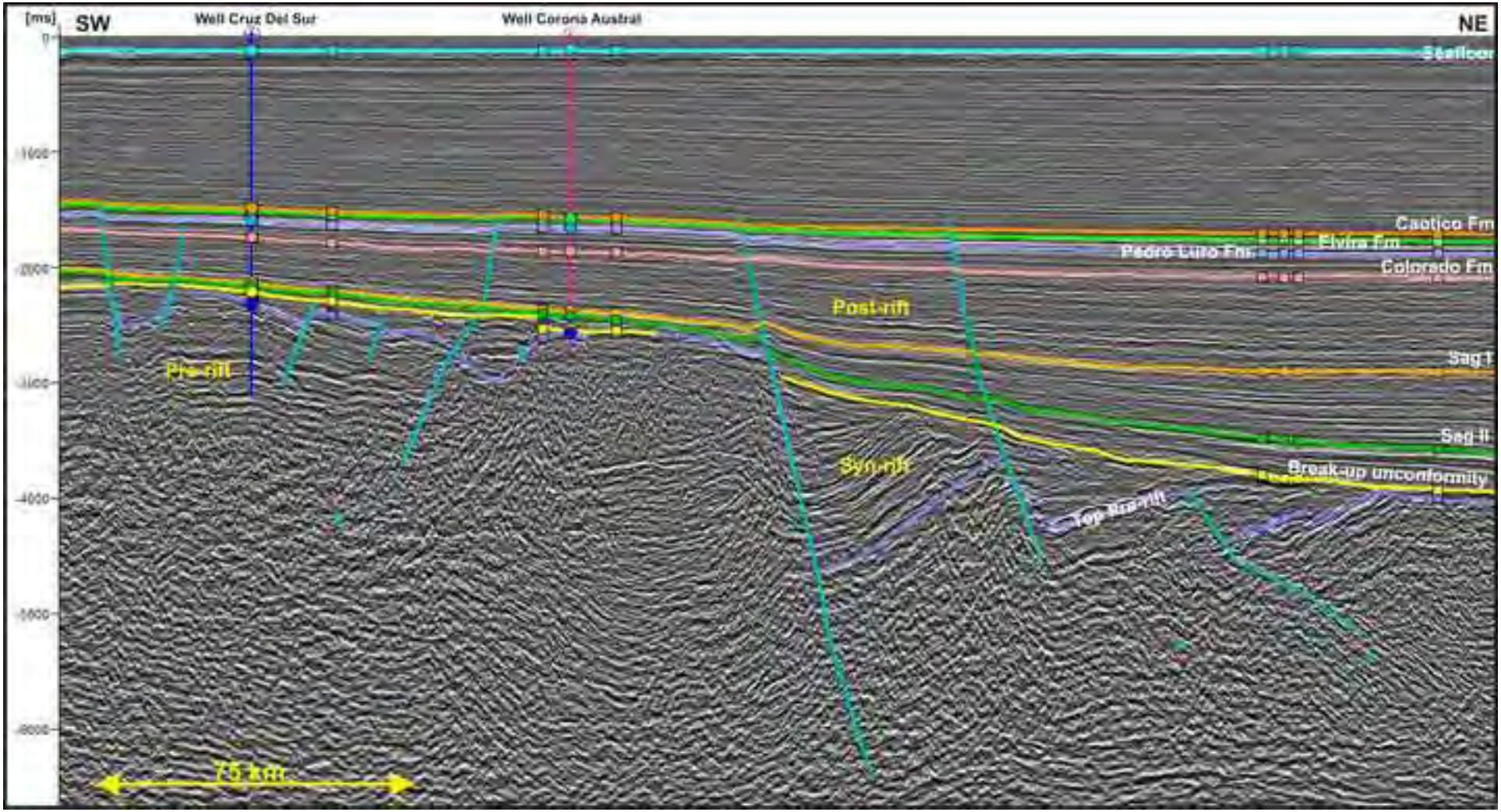

Figure 4ab

Click here to download high resolution image

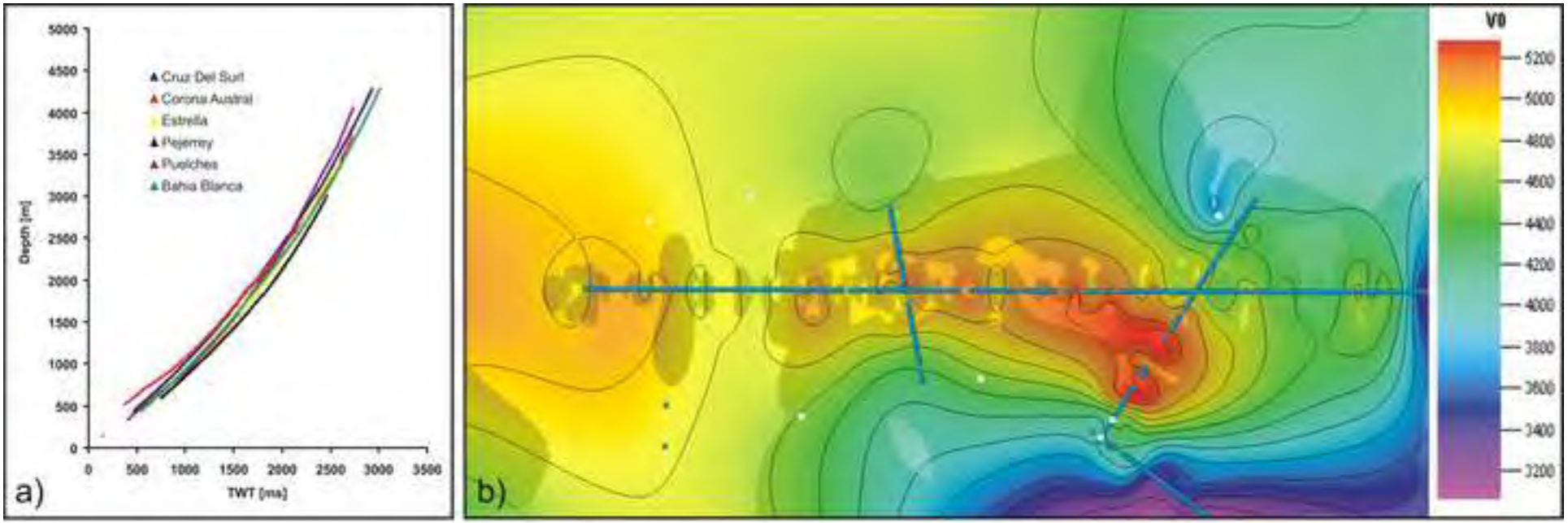

Figure 5

Click here to download high resolution image

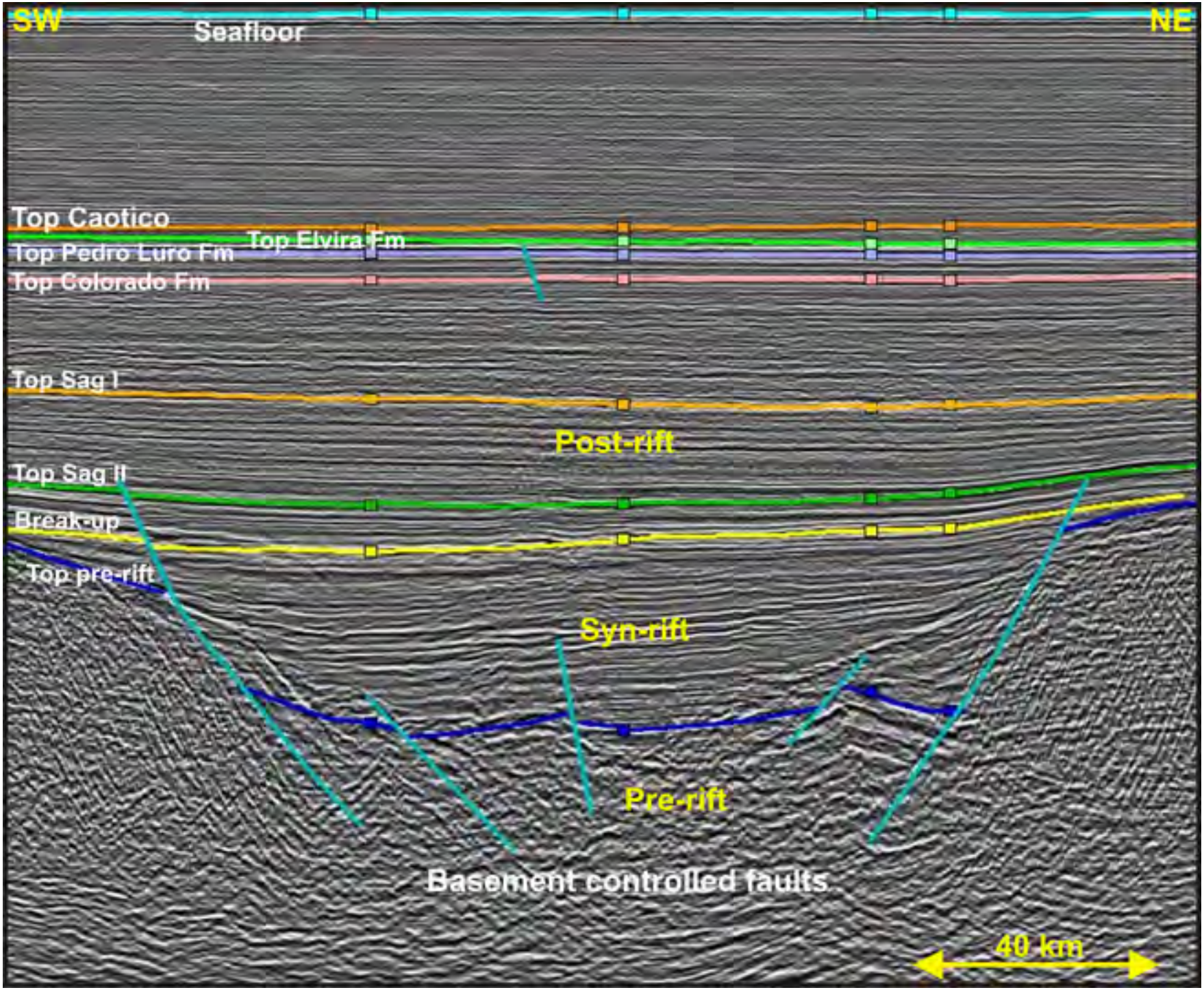

Figure 6

Click here to download high resolution image

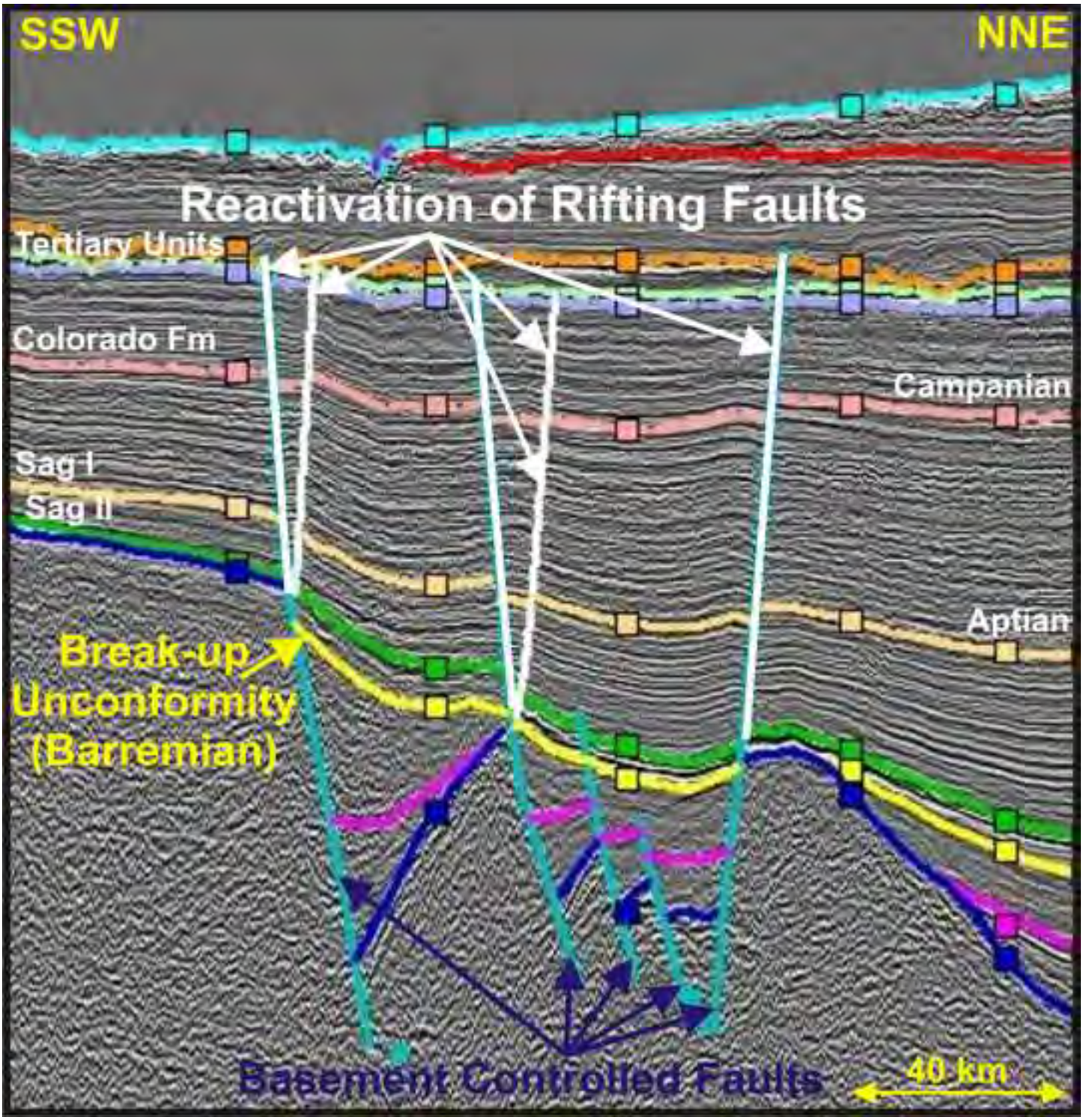

Figure 7

Click here to download high resolution image

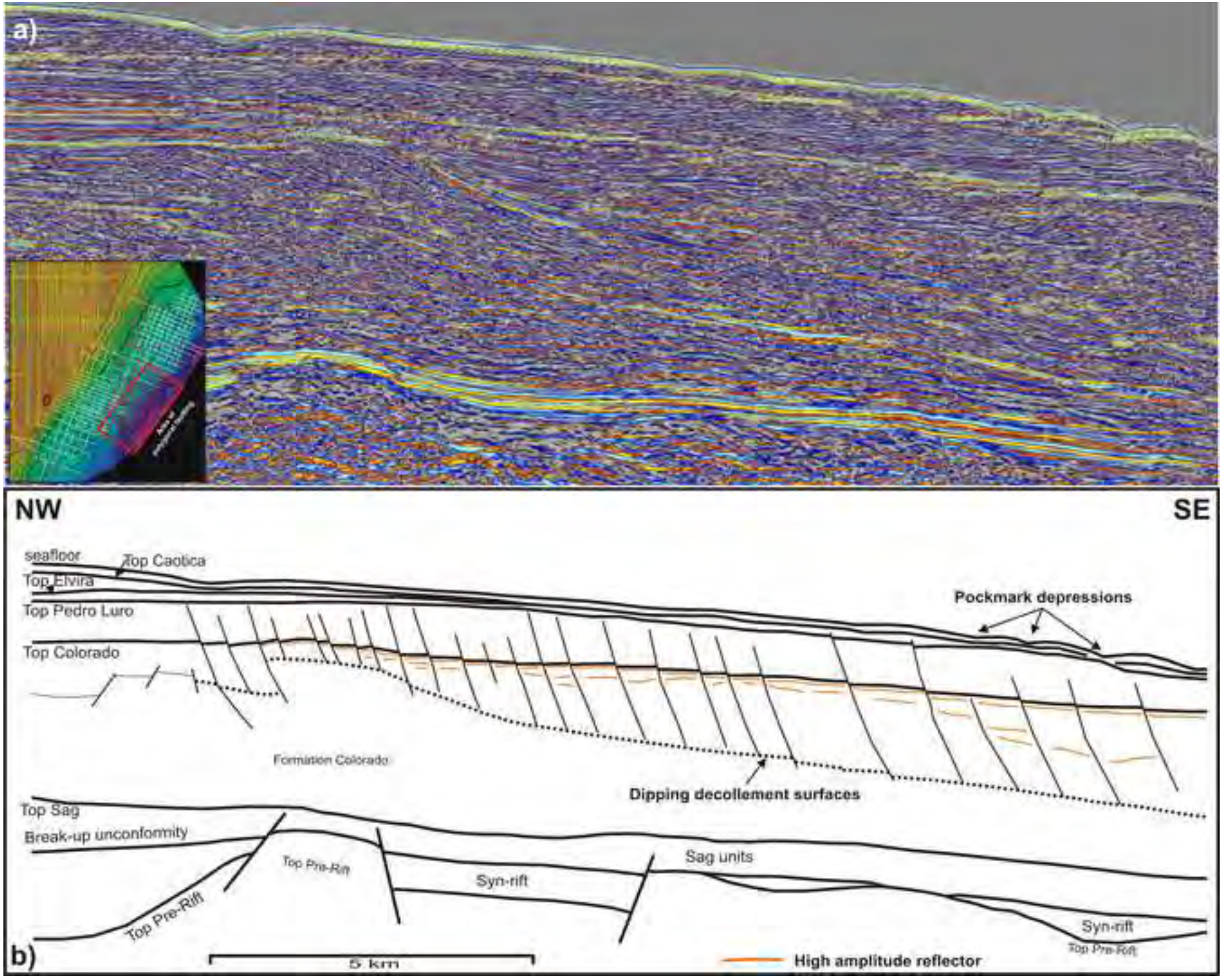

Figure 8

Click here to download high resolution image

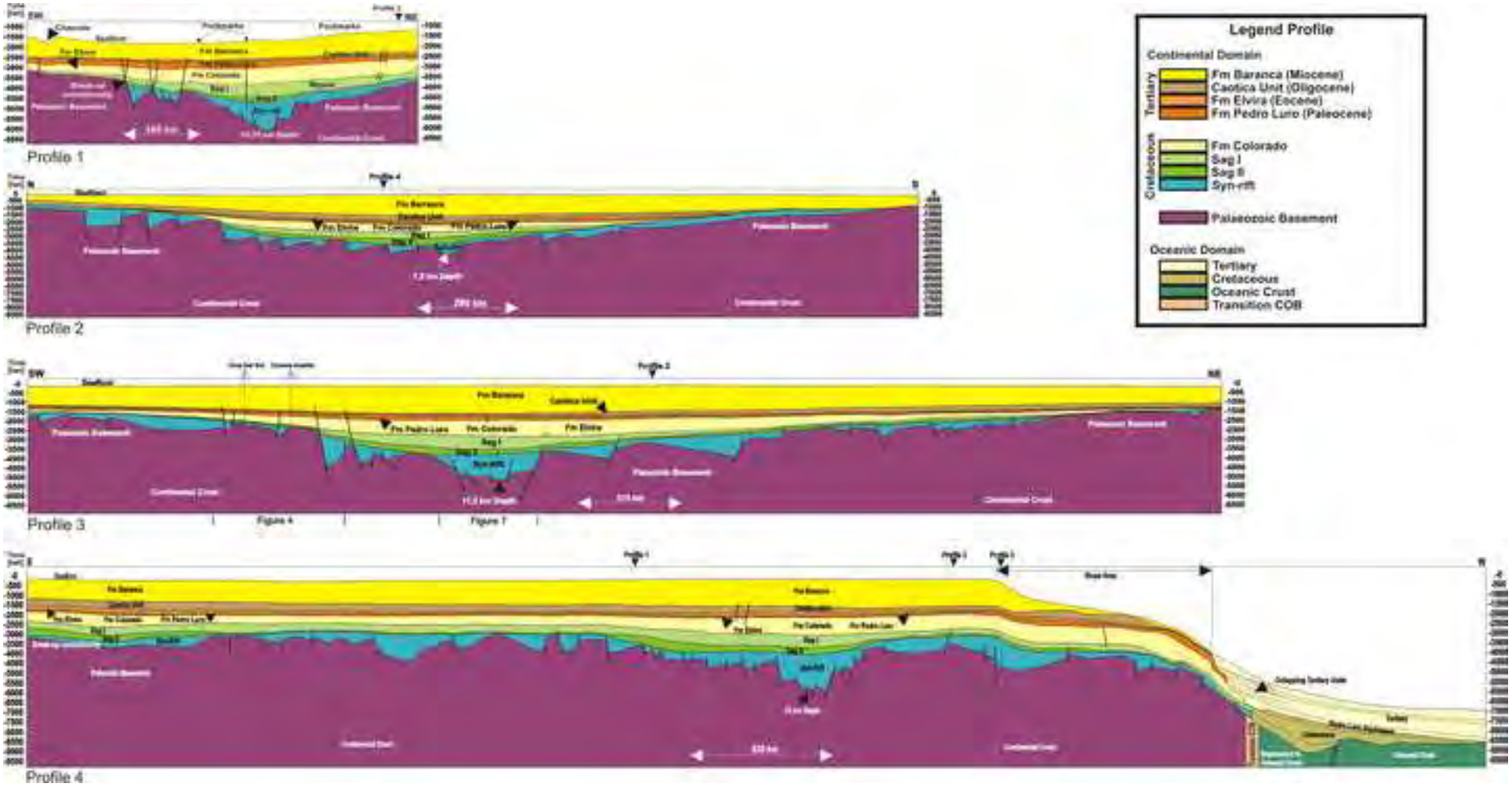

Figure 9a-i

Fig. 9a

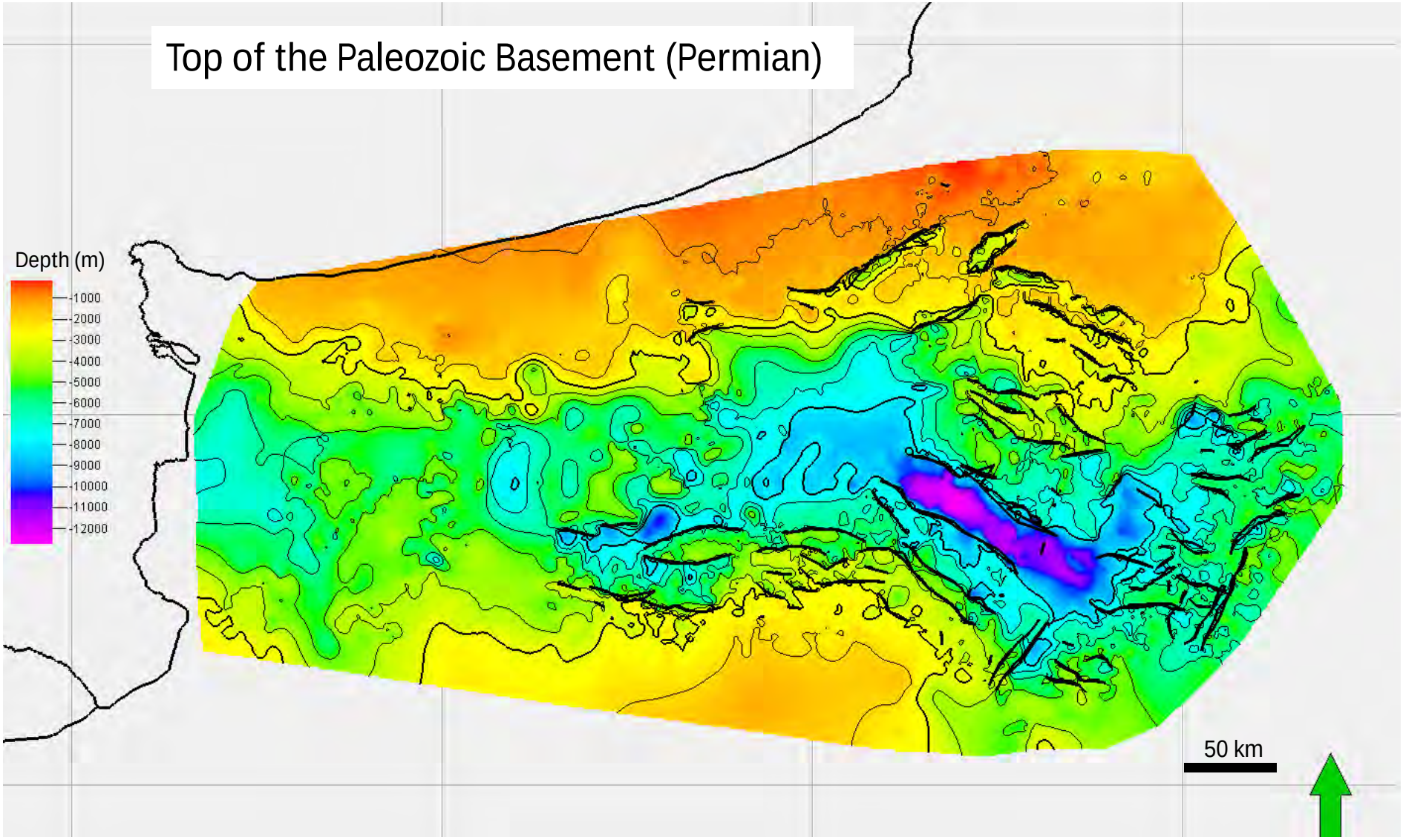

Fig. 9b

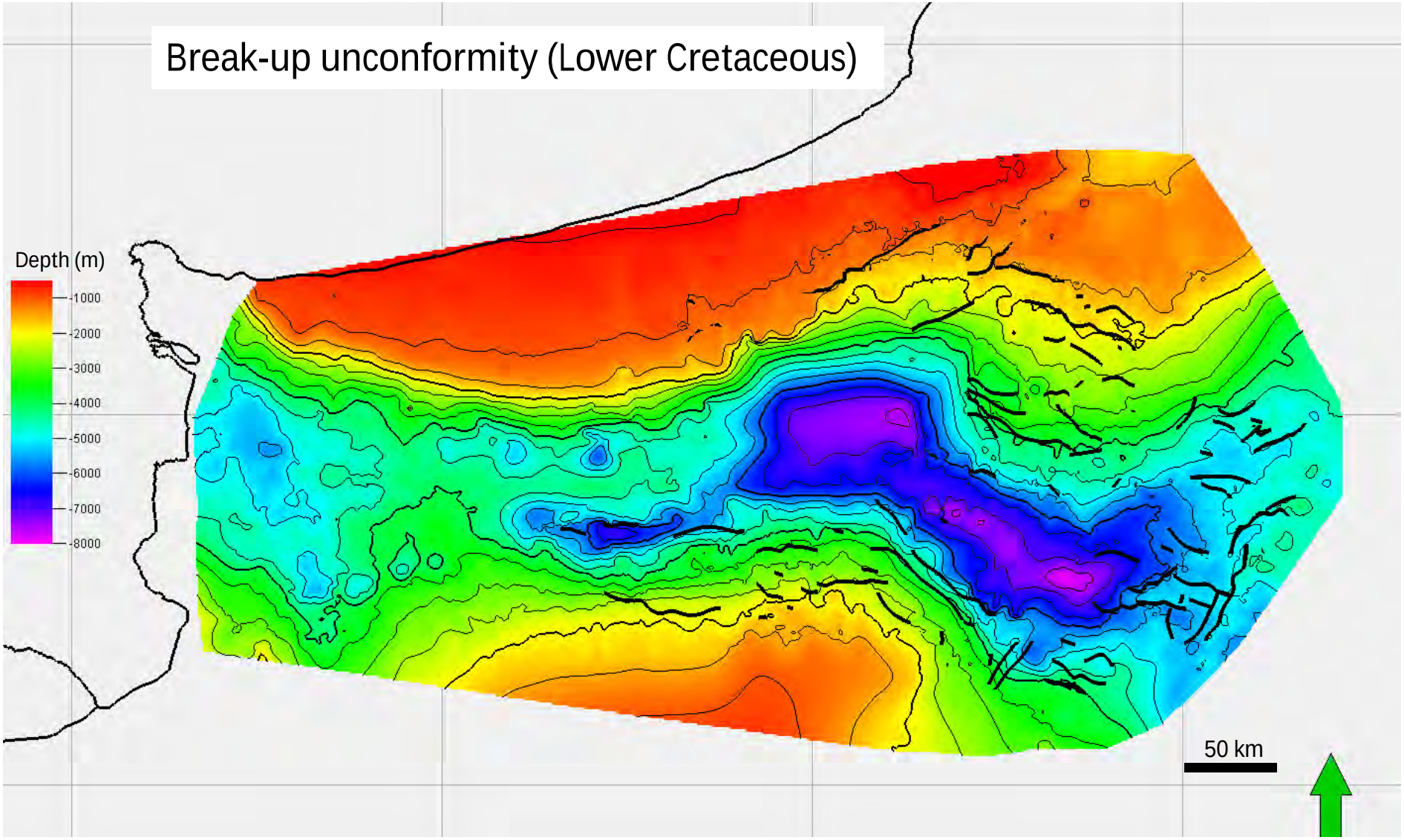
Break-up unconformity (Lower Cretaceous)
Depth (m)
-1000
-2000
-3000
-4000
-5000
-6000
-7000
-8000
50 km

Fig. 9c

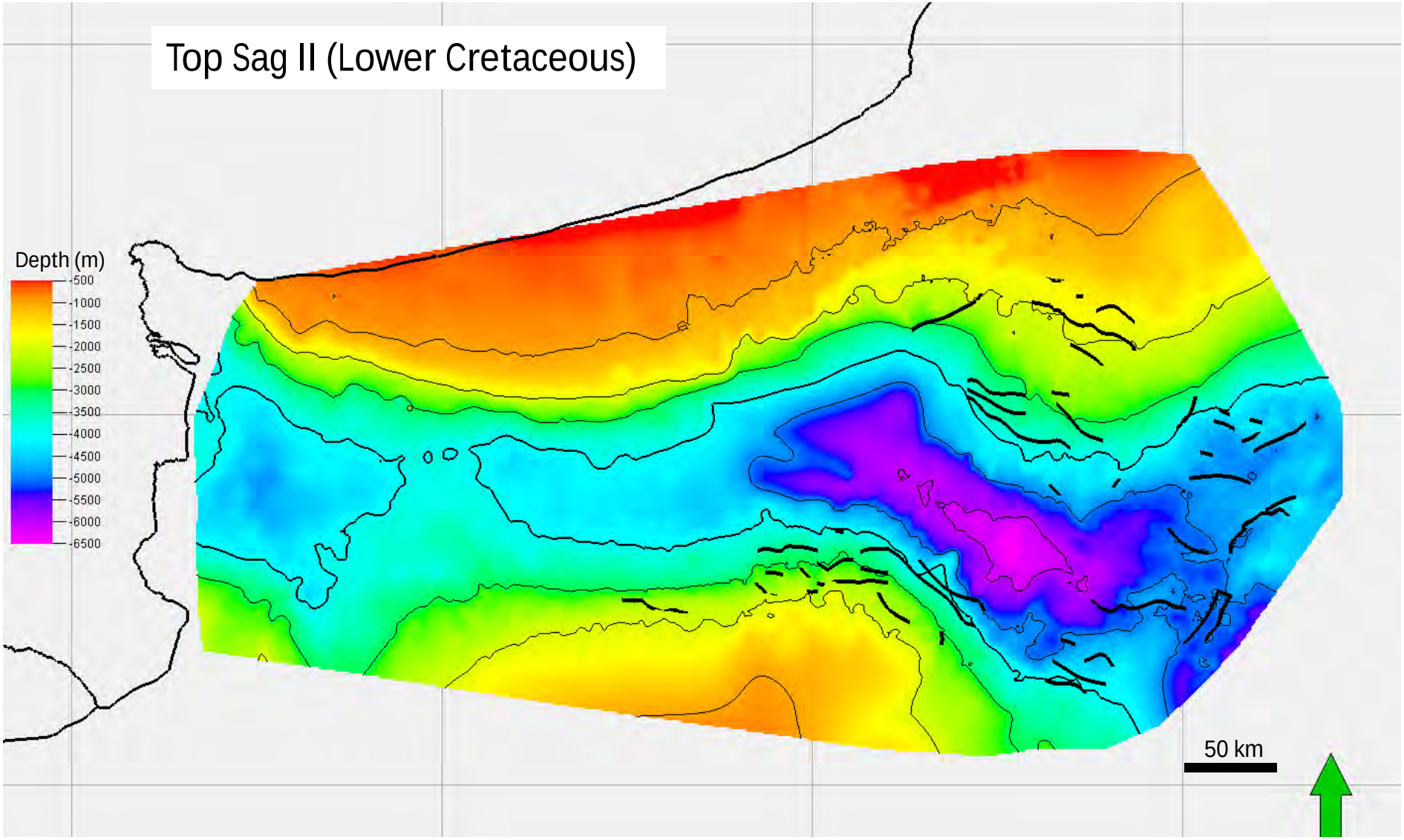
Top Sag II (Lower Cretaceous)
Depth (m)
-500
-1000
-1500
-2000
-2500
-3000
-3500
-4000
-4500
-5000
-5500
-6000
-6500
50 km

Fig. 9d

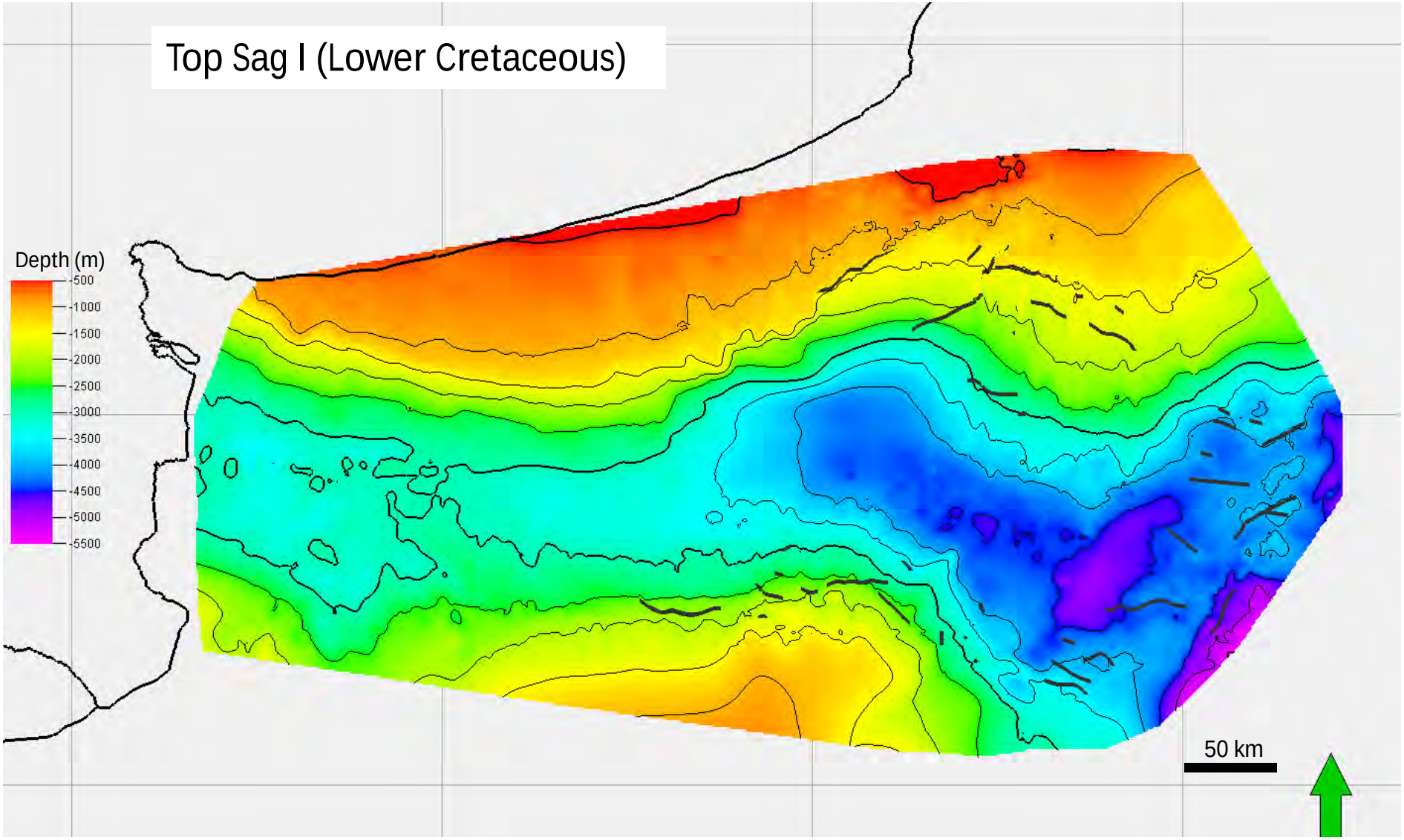
Top Sag I (Lower Cretaceous)
Depth (m)
-500
-1000
-1500
-2000
-2500
-3000
-3500
-4000
-4500
-5000
-5500
50 km

Fig. 9e

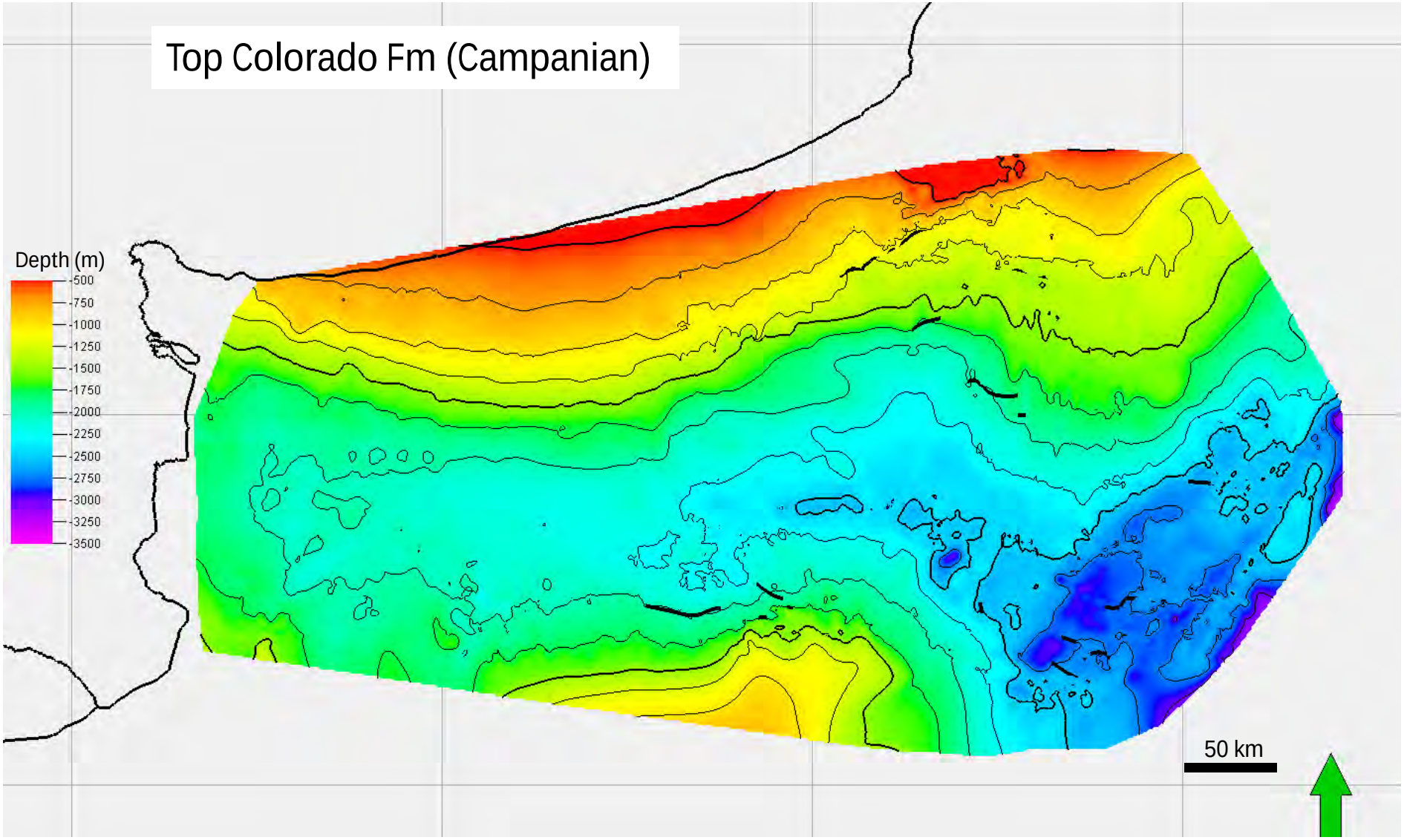
Top Colorado Fm (Campanian)
Depth (m)
-500
-750
-1000
-1250
-1500
-1750
-2000
-2250
-2500
-2750
-3000
-3250
-3500
50 km

Fig. 9f

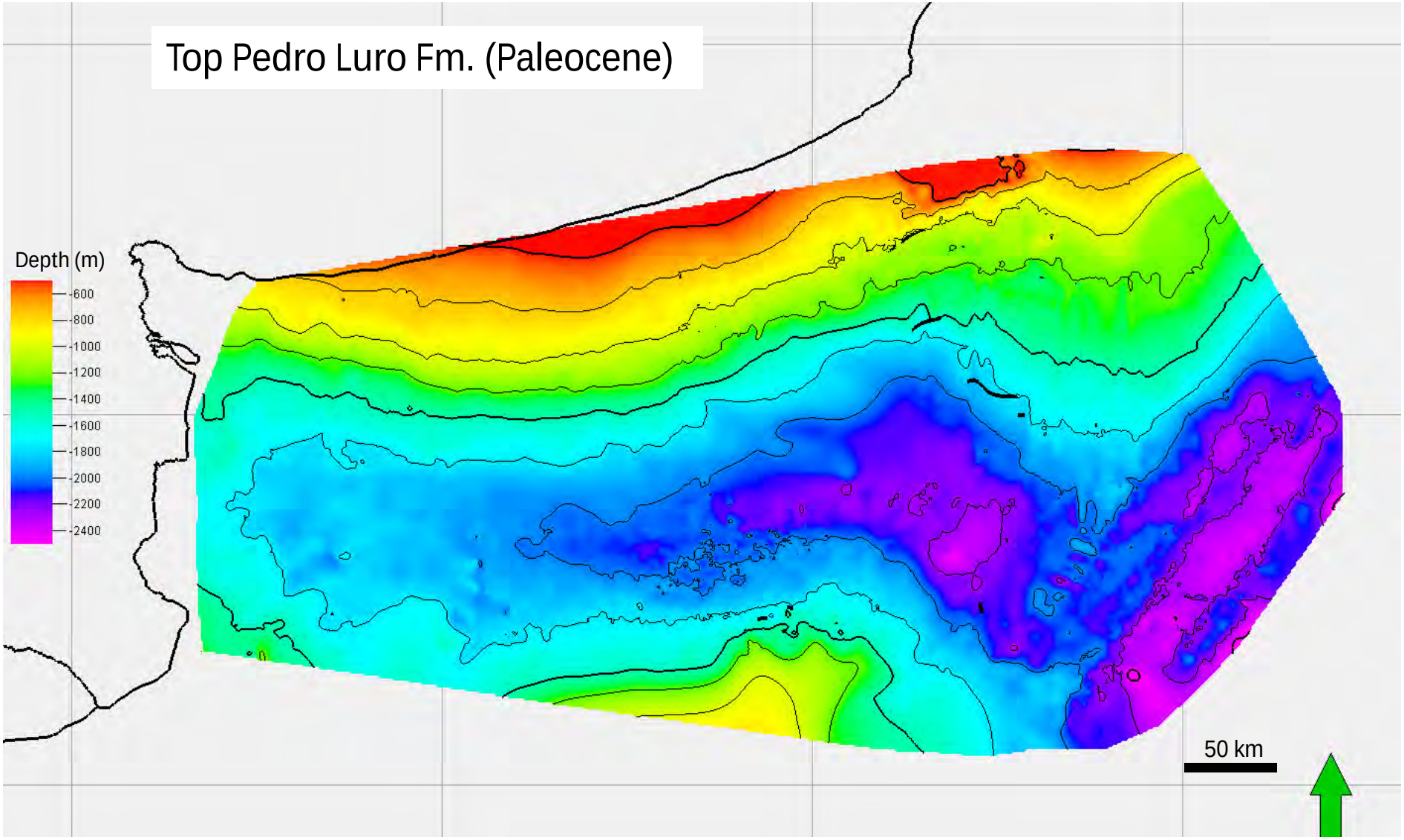
Top Pedro Luro Fm. (Paleocene)
Depth (m)
-600
-800
-1000
-1200
-1400
-1600
-1800
-2000
-2200
-2400
50 km

Fig. 9g

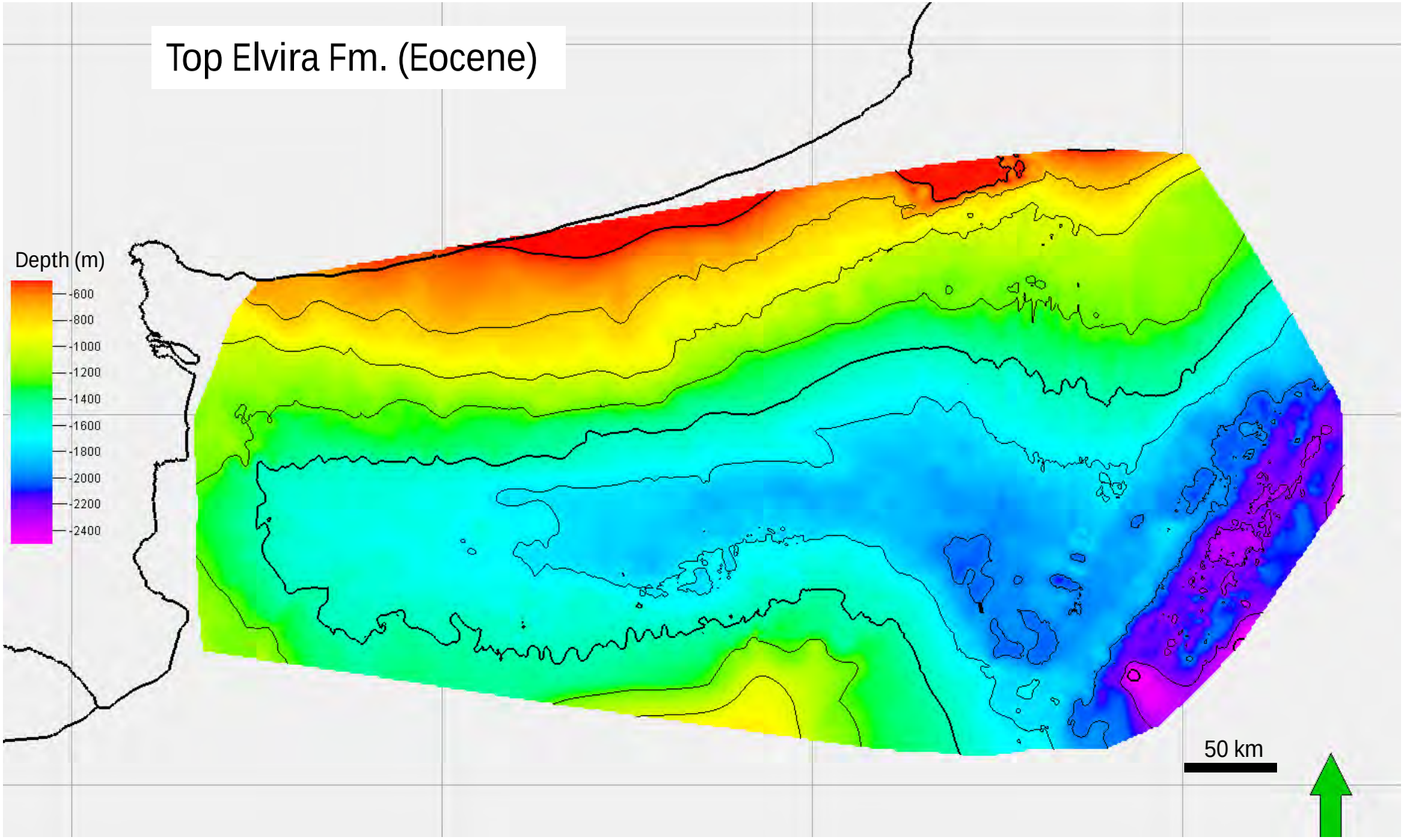
Top Elvira Fm. (Eocene)
Depth (m)
-600
-800
-1000
-1200
-1400
-1600
-1800
-2000
-2200
-2400
50 km

Fig. 9h

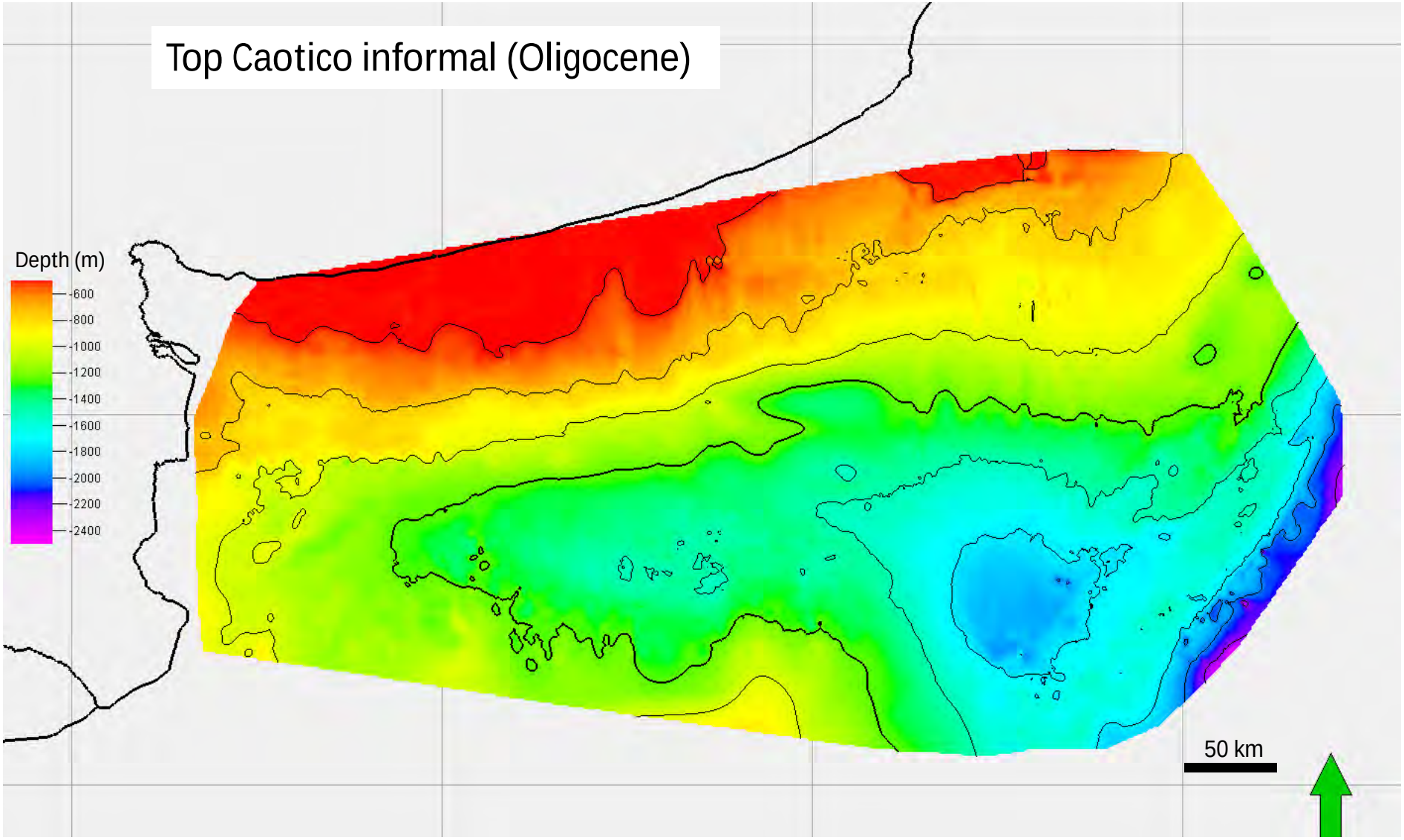
Top Caotico informal (Oligocene)
Depth (m)
-600
-800
-1000
-1200
-1400
-1600
-1800
-2000
-2200
-2400
50 km

Fig. 9i

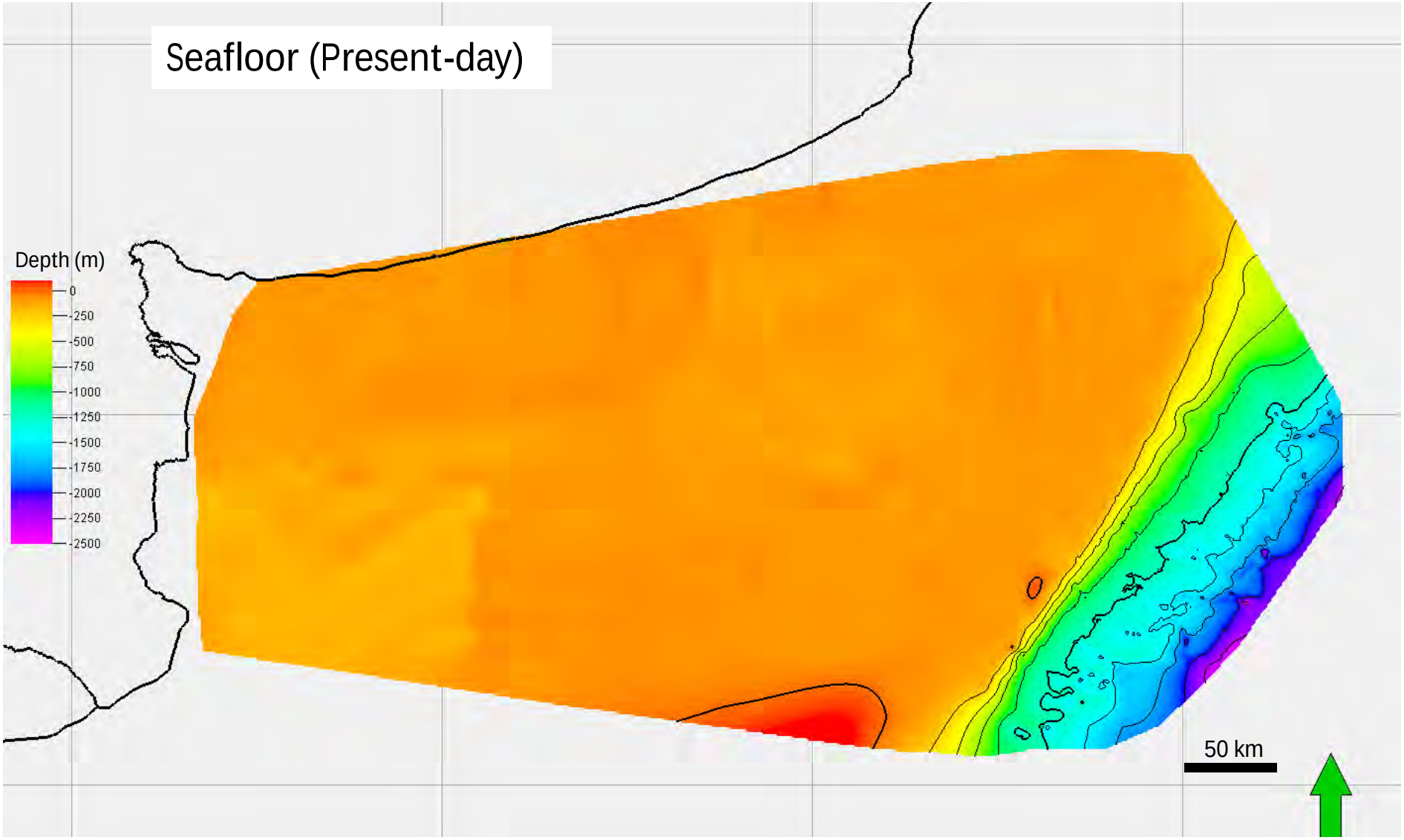
Seafloor (Present-day)
Depth (m)
0
-250
-500
-750
-1000
-1250
-1500
-1750
-2000
-2250
-2500
50 km

Figure 10a-h

Fig. 10a

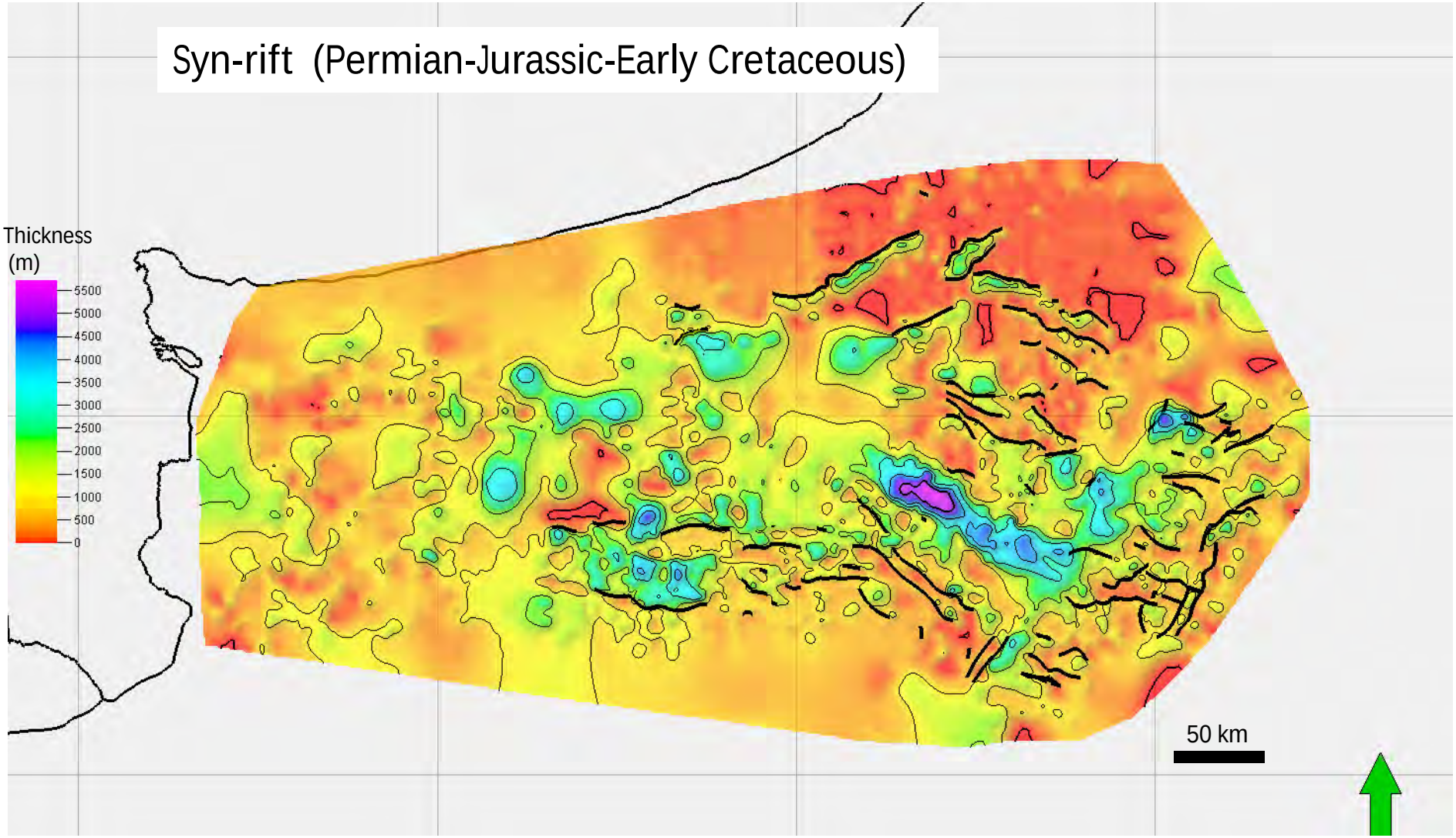

Fig. 10b

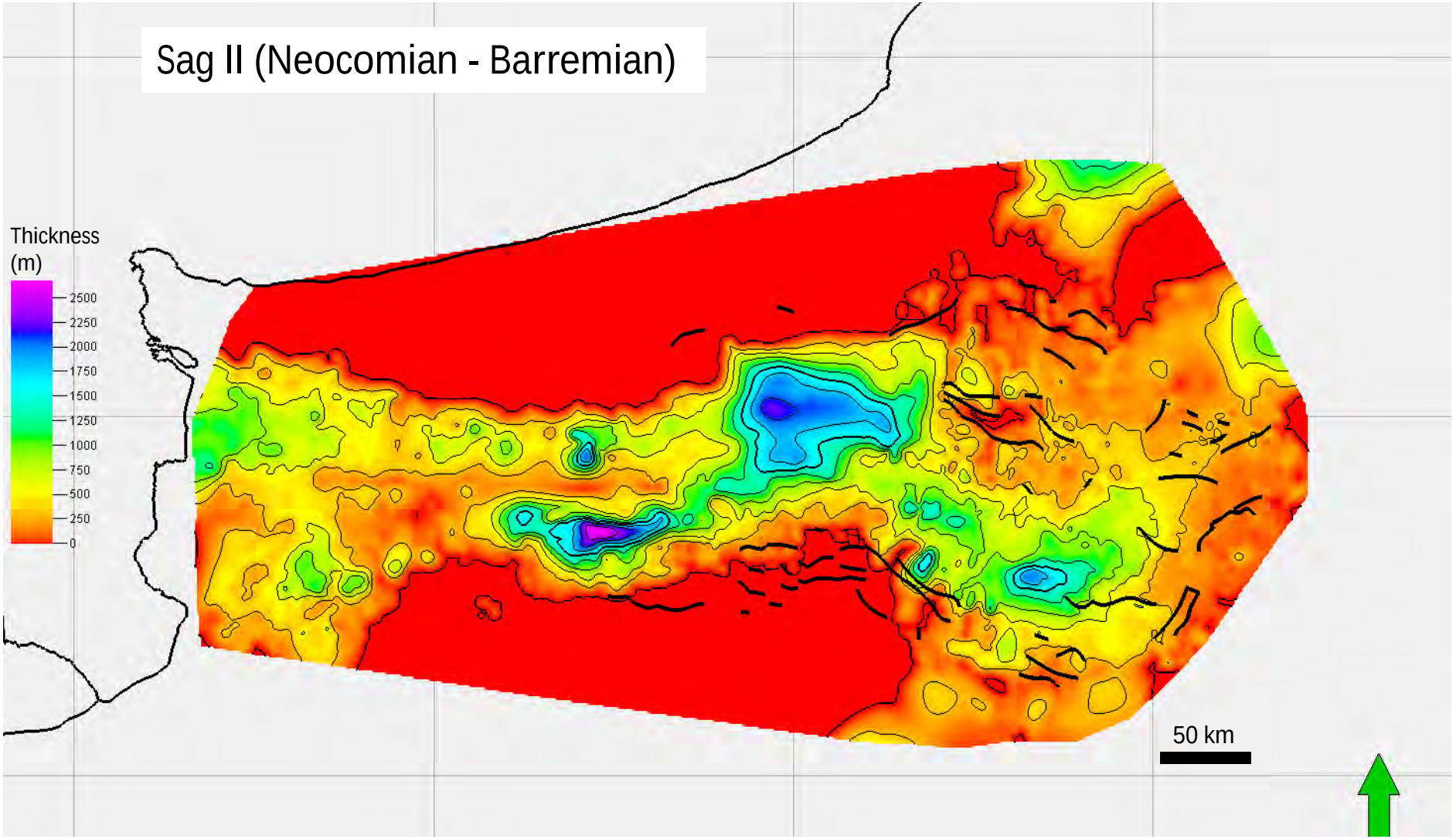
Sag II (Neocomian - Barremian)
Thickness (m)
2500
2250
2000
1750
1500
1250
1000
750
500
250
0
50 km

Fig. 10c

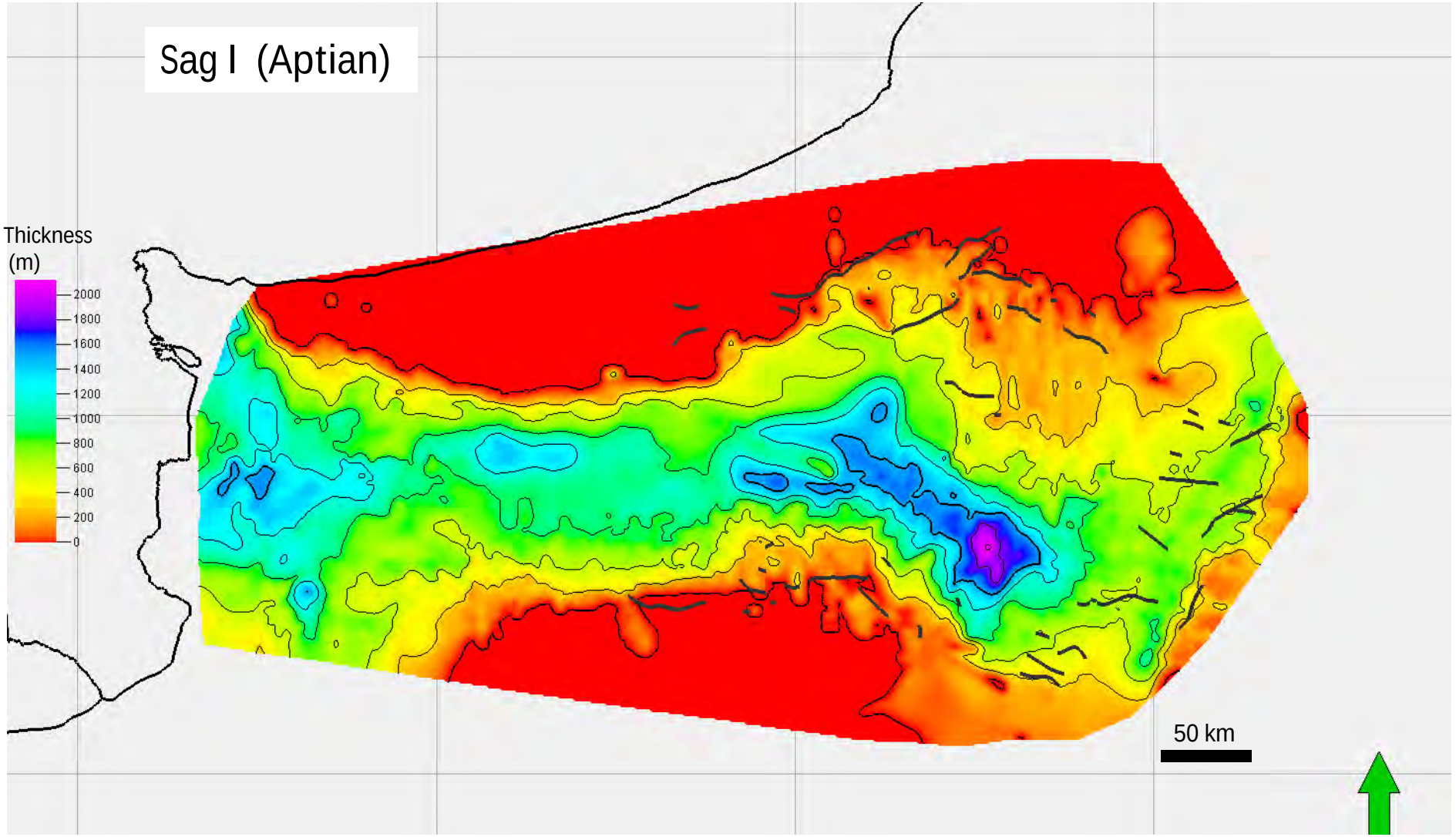
Sag I (Aptian)
Thickness
(m)
2000
1800
1600
1400
1200
1000
800
600
400
200
0
50 km

Fig. 10d

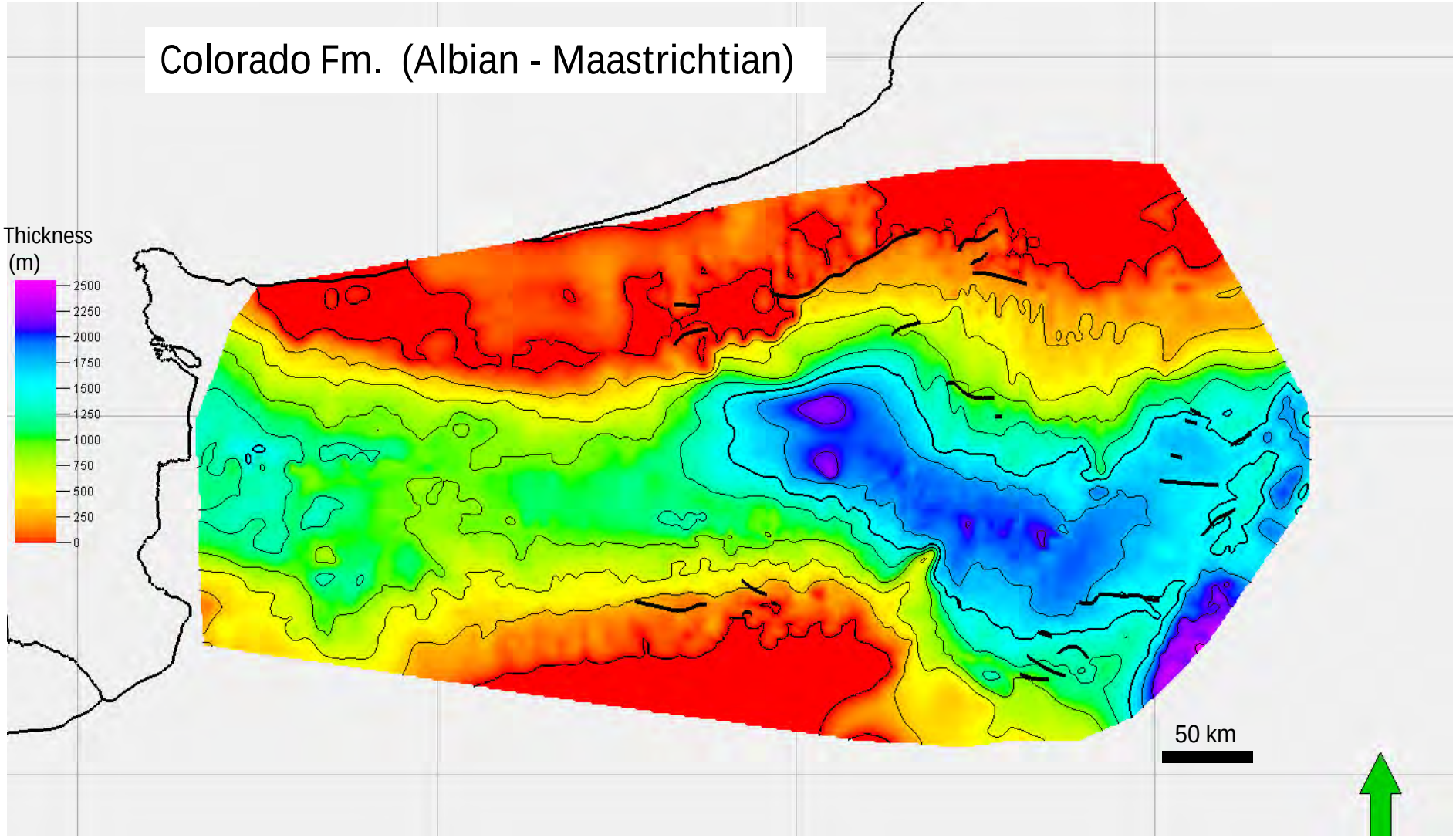
Colorado Fm. (Albian - Maastrichtian)
Thickness
(m)
2500
2250
2000
1750
1500
1250
1000
750
500
250
0
50 km

Fig. 10e

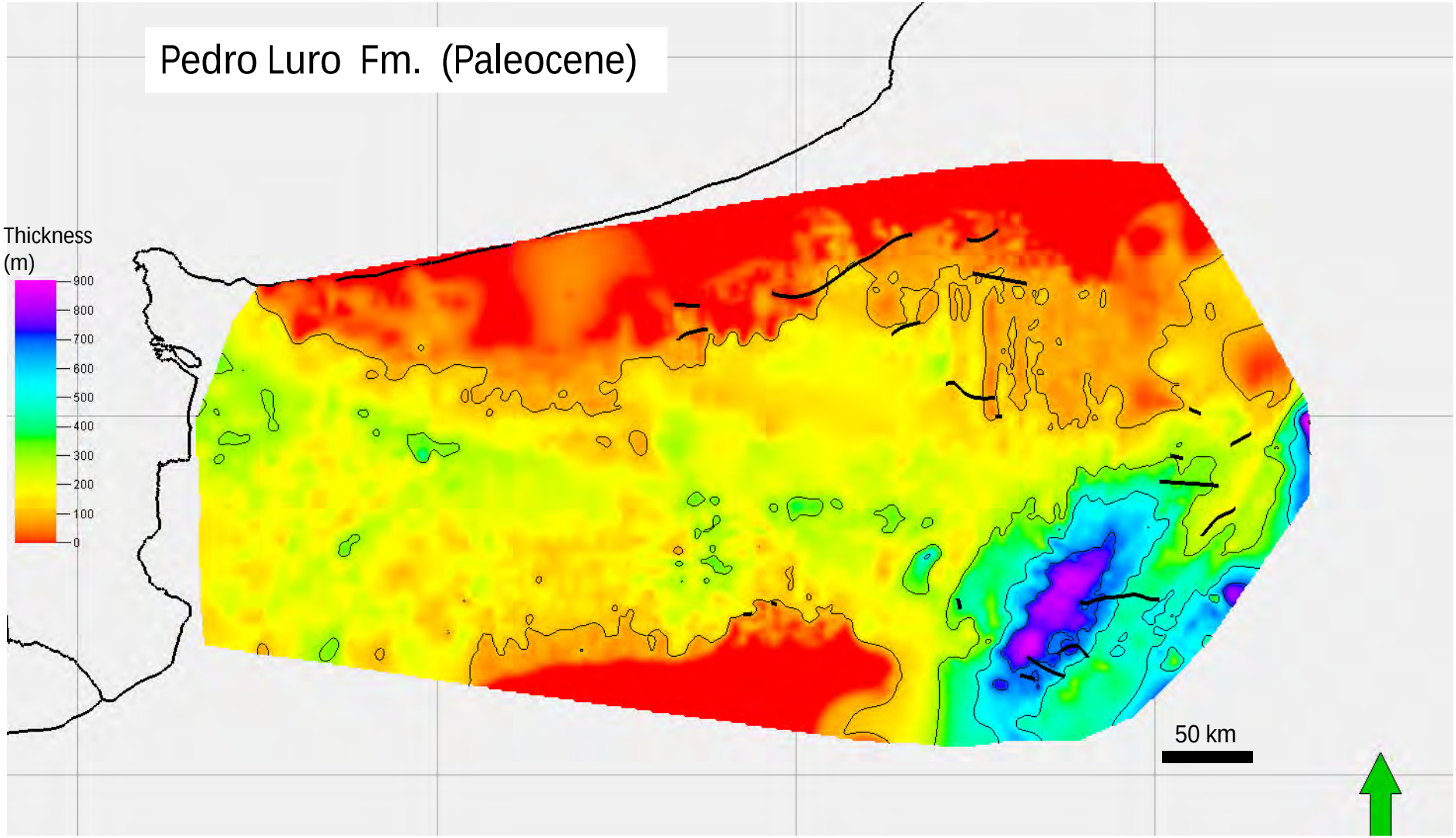
Pedro Luro Fm. (Paleocene)
Thickness (m)
900
800
700
600
500
400
300
200
100
0
50 km

Fig. 10f

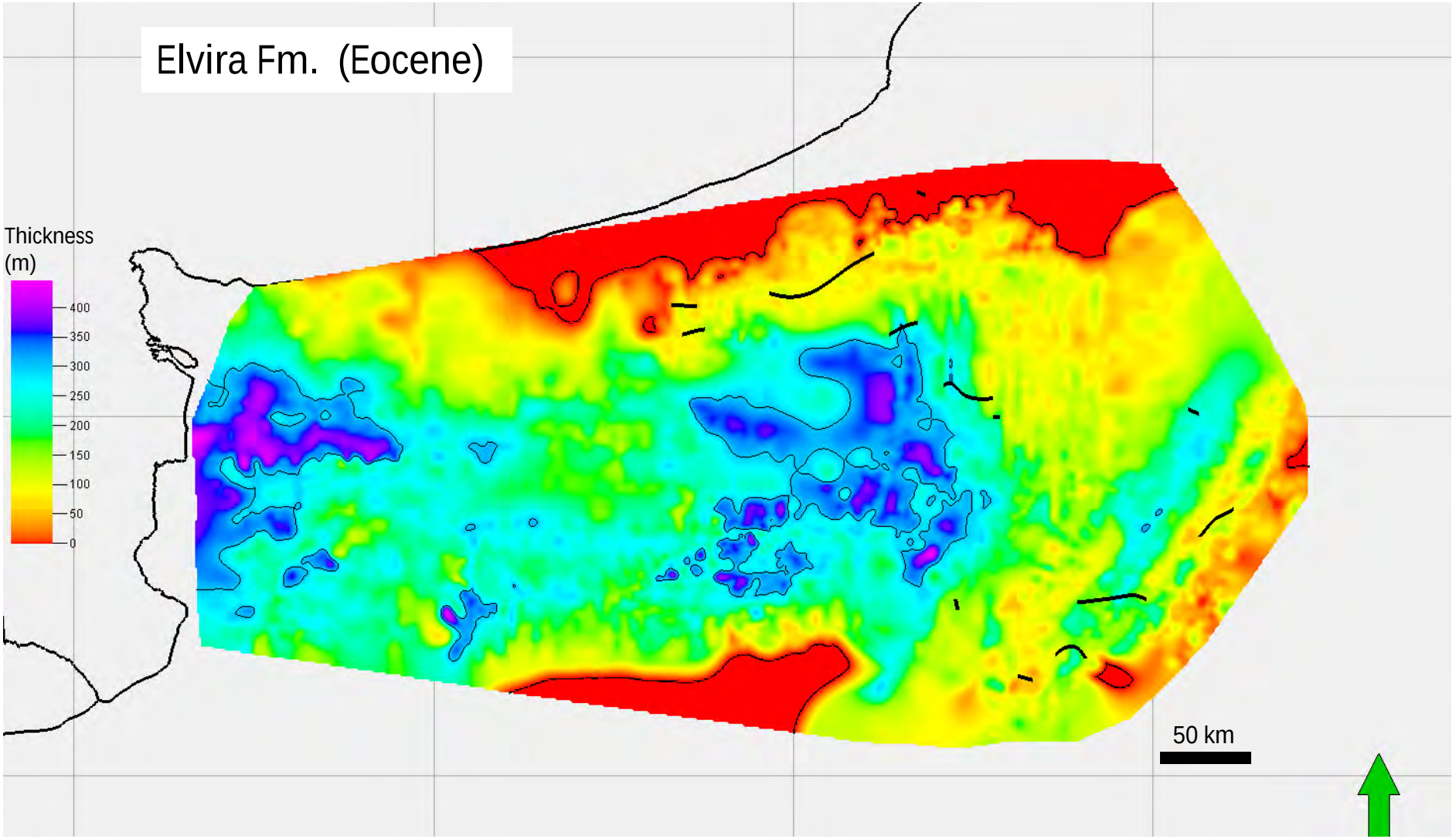
Elvira Fm. (Eocene)
Thickness
(m)
400
350
300
250
200
150
100
50
0
50 km

Fig. 10g

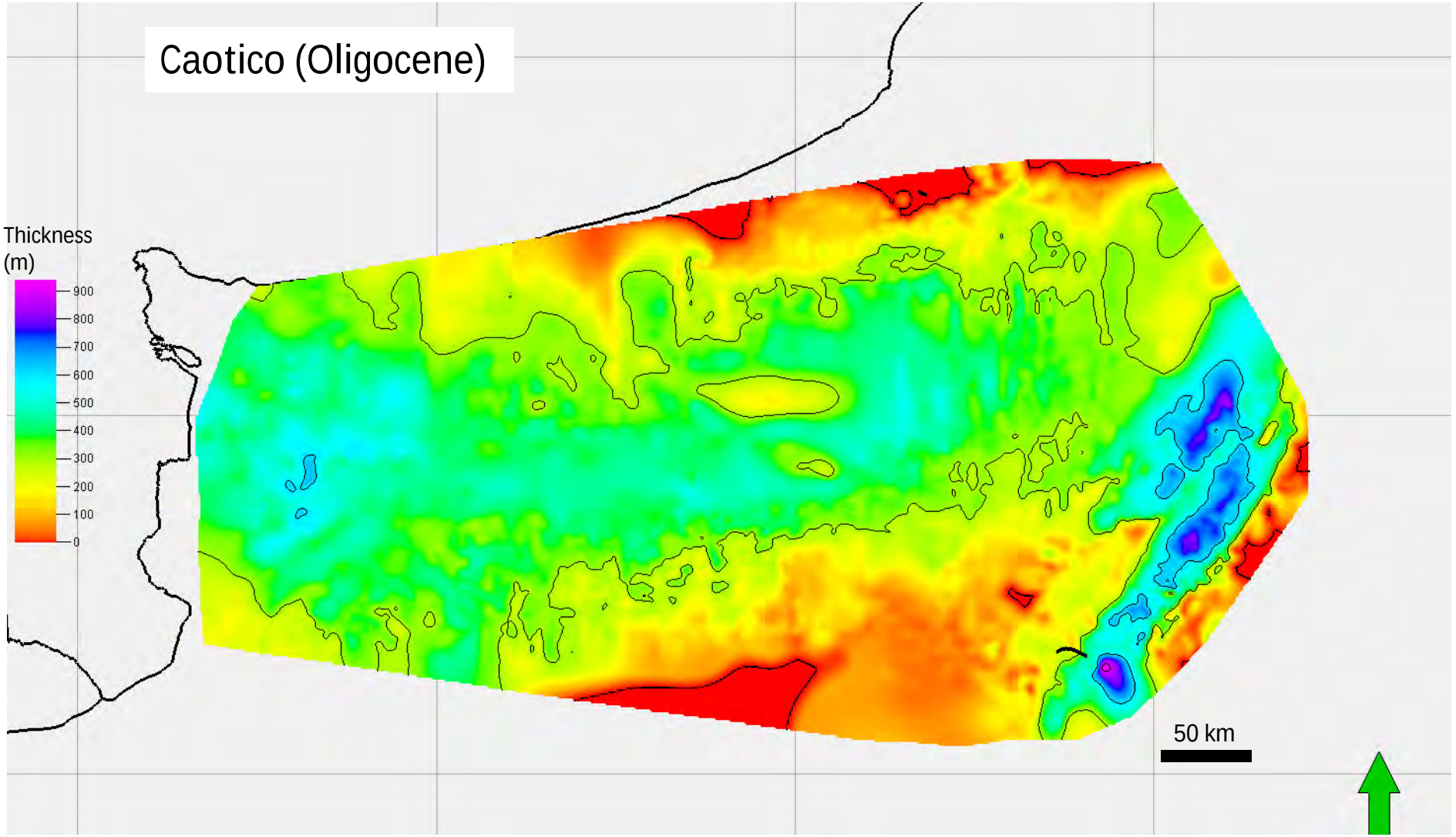
Caotico (Oligocene)
Thickness
(m)
900
800
700
600
500
400
300
200
100
0
50 km

Fig. 10h

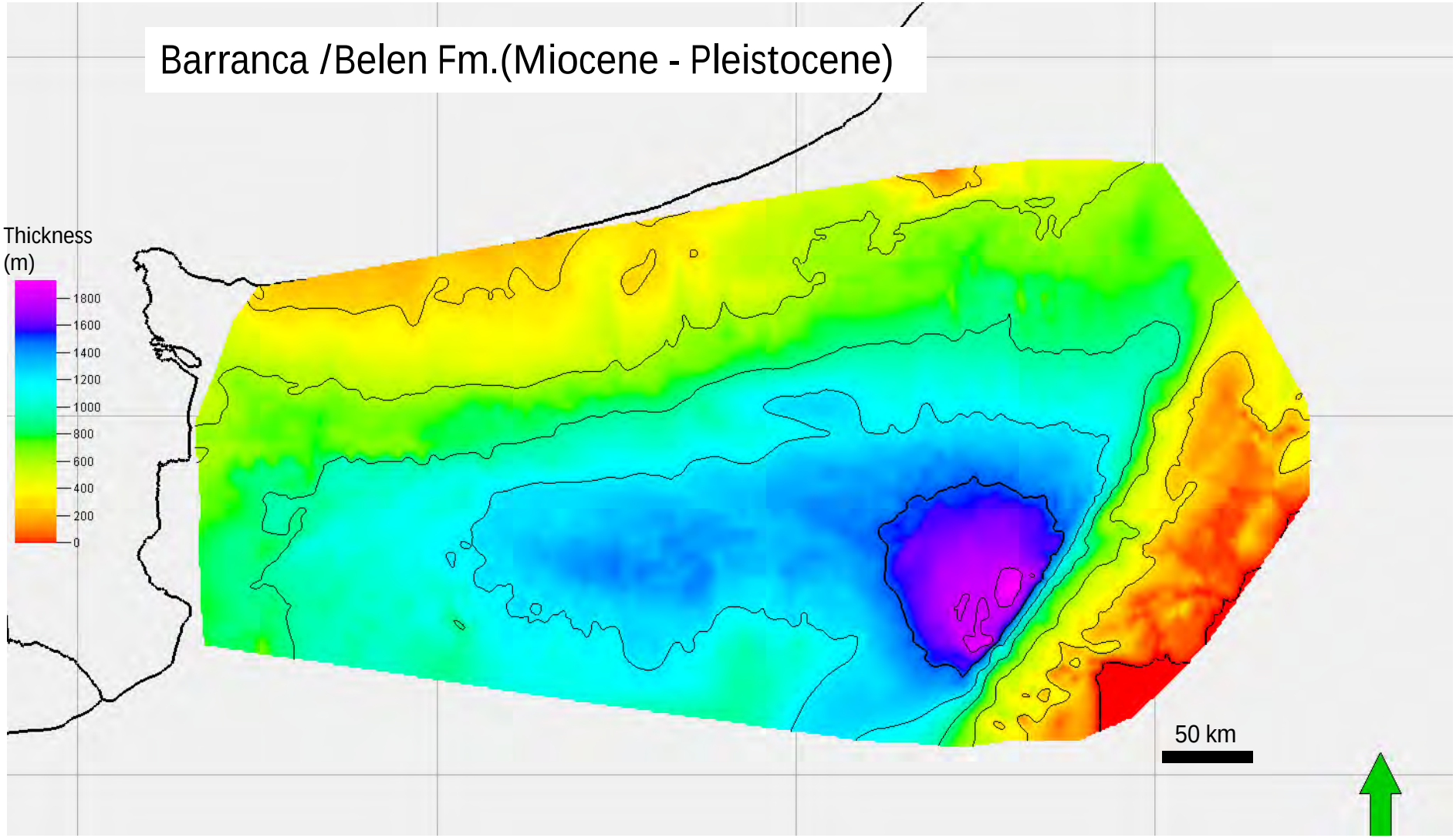
Barranca /Belen Fm.(Miocene - Pleistocene)
Thickness
(m)
1800
1600
1400
1200
1000
800
600
400
200
0
50 km

Figure 11

Click here to download high resolution image

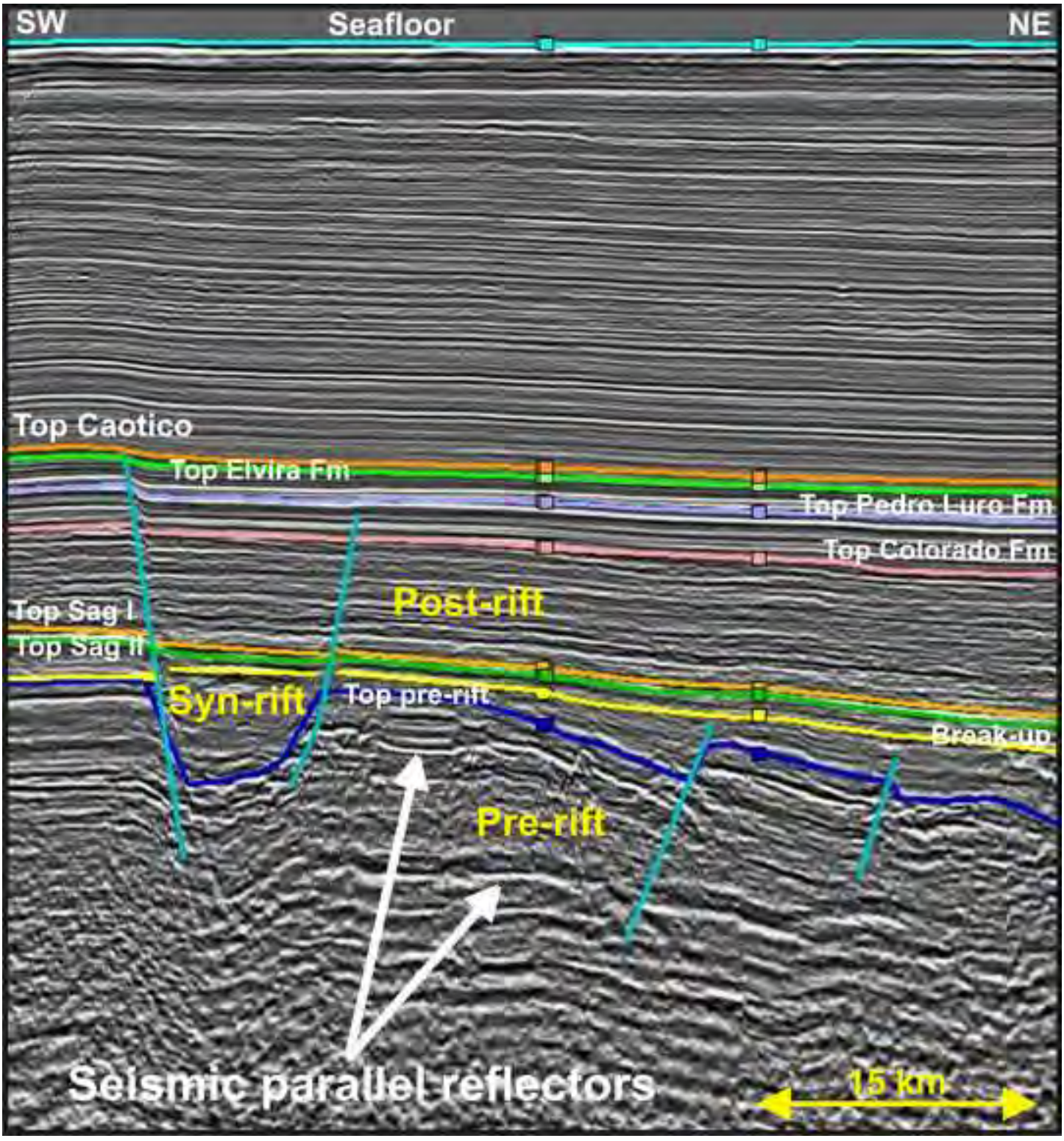

Figure 12

Click here to download high resolution image

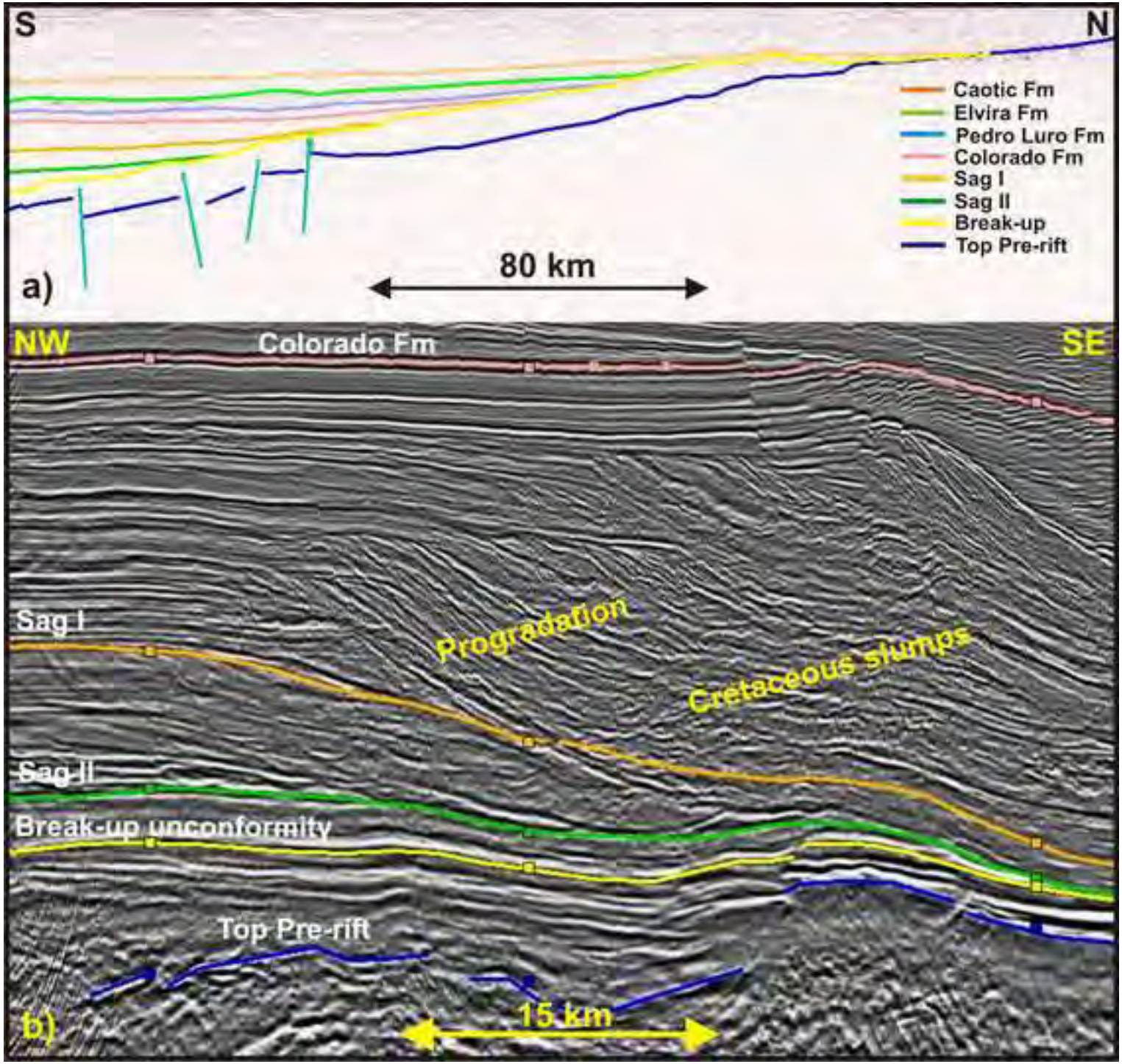

Figure 13

Click here to download high resolution image